1990

Red and orange fluorescence and beam attenuation to intermediate depths in the Northeast Pacific Ocean

Marilyn Ann Yuen
San Jose State University

Order Number 1342743

Red and orange fluorescence and beam attenuation to intermediate depths in the Northeast Pacific Ocean

Yuen, Marilyn Ann, M.S.

San Jose State University, 1990

U·M·I
300 N. Zeeb Rd.
Ann Arbor, MI 48106

RED AND ORANGE FLUORESCENCE AND BEAM ATTENUATION TO INTERMEDIATE DEPTHS IN THE NORTHEAST PACIFIC OCEAN

A Thesis

Presented to

The Faculty of Moss Landing Marine Laboratories

San Jose State University

In Partial Fulfillment

of the Requirements for the Degree

Master of Science

in

Marine Science

By

Marilyn Ann Yuen

December 1990

APPROVED FOR MOSS LANDING MARINE LABORATORIES

William Broenkow

Dr. William W. Broenkow

Kenneth S Johnson

Dr. Kenneth S. Johnson

Nicholas A. Welschmeyer

Dr. Nicholas A. Welschmeyer

APPROVED FOR THE UNIVERSITY

Serena M. Stanford

ABSTRACT

RED AND ORANGE FLUORESCENCE AND BEAM ATTENUATION TO INTERMEDIATE DEPTHS IN THE NORTHEAST PACIFIC OCEAN

by Marilyn Ann Yuen

Continuous profiles to 2000 m of red (chlorophyll) and orange (phycoerythrin) fluorescence and beam attenuation were obtained between 33° and 59° N in the Northeast Pacific Ocean. Near-surface maxima in these properties were prominent in the Gulf of Alaska. The strong, shallow orange fluorescence signal suggests that the occurrence of phycoerythrin containing organisms, probably cyanobacteria, is more widespread than previously reported. The underlying chlorophyll fluorescence minimum (~200-300 m) was conspicuous in oligotrophic central gyre waters but limited in eutrophic subarctic waters; the corresponding phycoerythrin fluorescence minimum was prevalent throughout the section. These differences in the fluorescence minima indicate that different processes are involved in the production and degradation of chlorophyll and phycoerythrin containing particles. The tertiary fluorescence maxima (~1000 m) were continuous throughout the Northeast Pacific Ocean. The phycoerythrin fluorescence maximum at depth suggests the presence of heterotrophic cyanobacteria, an hypothesis as yet unsupported by biological evidence.

ACKNOWLEDGEMENTS

The accomplishment of this thesis would not have been possible without the advice and support of many people. I am indebted to Dr. William Broenkow for teaching me how to distinguish the forest from the trees. Drs. Kenneth Johnson and Nicholas Welschmeyer were always helpful with timely discussions and suggestions. I appreciate the efforts of Sheila Baldridge and Sandi O'Neil in obtaining many references for me over the years. Lynn McMasters generously helped me prepare many of the final figures.

I am most fortunate to have learned from the experience and patience of Mark Yarbrough. Mark is largely responsible for molding a naive and inexperienced person into a competent, seaworthy technician. I am grateful for the technical expertise of Richard Reaves, who has shown me many tricks towards mastering a computer.

I am lucky to have been surrounded by so many wonderful friends during my tenure here. Moral support was generously given by Eric Dorfman, Ronnie Estelle, Andy and Janet Heard, Susan McBride, Guillermo Moreno, Cathy Rathbun, Sara Tanner, Cary and Claire Wong, Debbie Wyatt, and Mark and Sandy Yarbrough. The efforts and understanding of Susan Dearn and Melanie Mayer during the final throes of "thesis fever" are appreciated as well.

Special thanks go to Dr. Giacomo DiTullio for his encouragement and helpful comments, as well as his moral and emotional support, during the writing process and the thesis defense.

Last, but not least, I appreciate the opportunities afforded me by Dr. John Martin and the faculty and staff of Moss Landing Marine Laboratories. The program and environment they provided was an outstanding experience for me.

This research was supported by the National Science Foundation Marine Chemistry Program, Grant No. OCE-86-00456 to Dr. William Broenkow, and by the Office of Naval Research Ocean Chemistry Program, Grant No. N 000 14-84-C-0619 to Dr. John Martin.

TABLE OF CONTENTS

LIST OF FIGURES

Figure

Page

LIST OF TABLES

INTRODUCTION

With the advent of *in situ* instrumentation in the early 1960's, small-scale oceanographic features that were previously excluded by bottle and net sampling were revealed. High resolution data from *in situ* fluorometers and beam transmissometers increased the understanding of oceanic phytoplankton ecology; however, prior to the work of Broenkow *et al.* (1983), *in situ* fluorometry was restricted to the euphotic zone. During the VERtical Transport and EXchange (VERTEX) program (Martin *et al.*, 1983), *in situ* fluorescence was measured to intermediate depths (1500 m) for the first time.

Observations in the eastern tropical Pacific Ocean showed the presence of three fluorescence maxima (Broenkow *et al.*, 1983). The well known primary maximum near 50 m is associated with euphotic zone phytoplankton (Anderson, 1969; Venrick *et al.*, 1973). The secondary maximum near 100 m was only observed off of Mexico at the interface between the surface waters and the underlying, nearly anoxic waters. The hypothesis that this feature is due to nitrifying bacteria (Lewitus and Broenkow, 1985) has been supported by recent work off the coast of Peru (Spinrad *et al.*, 1989). The broad tertiary maximum appeared at intermediate depths (1000 m) near the core of the oxygen minimum zone. Spectral investigation of the tertiary fluorescence maximum yielded the following potential

fluorescent pigments as the source of the fluorescence signal: chlorophyll *a* (685 nm) and its degradation products from phytoplankton; phycoerythrin (570-590 nm) from cyanobacteria and cryptomonads; and bacteriochlorophylls (>700 nm) from purple non-sulfur bacteria (Broenkow *et al.*, 1985).

Direct observations of *in situ* fluorescence and total attenuation lead to indirect observations regarding the distribution of organisms involved in photosynthesis, aphotic oxygen consumption, nutrient regeneration and consumption, and dissolved organic carbon consumption. The purpose of this study was to increase our knowledge of the spatial extent of these fluorescence maxima, thereby providing more extensive indirect observations for hypotheses concerning their origin.

METHODS

During 26 July to 14 August 1987, continuous profiles to 2000 m of conductivity, temperature, dissolved oxygen, total attenuation, and red and orange fluorescence were obtained in a 3000 km transect from 33° N, 139° W to 60° N, 149° W (Fig. 1). The section consisted of 16 optical CTDO (conductivity, temperature, depth, oxygen) stations (Table 1), of which six included trace metal work (Martin *et al.*, 1989). A minimum of two CTDO profiles were acquired at each trace metal station, but only one for each of the others. The CTDO system used during the VERTEX 7 cruise incorporated a Sea-Bird SBE-4 conductivity cell, a Plessey platinum temperature transducer, a Digiquartz 46K-02 pressure transducer, a modified Beckman polarographic oxygen electrode, a modified Martek beam transmissometer, and a modified *in situ* Variosens II fluorometer (Yarbrough *et al.*, 1989).

All raw profile data were converted and corrected by applying lab and/or field calibrations (Table 2). At selected depths, the CTDO rosette with 2.5 liter sampling bottles was used to collect field calibrations for salinity, temperature, dissolved oxygen, and chlorophyll *a*. Salinity samples were analyzed ashore using a Guildline Autosal 8400 standardized with standard seawater, and conductivity was converted to salinity according to the SCOR-UNESCO (1981) equations.

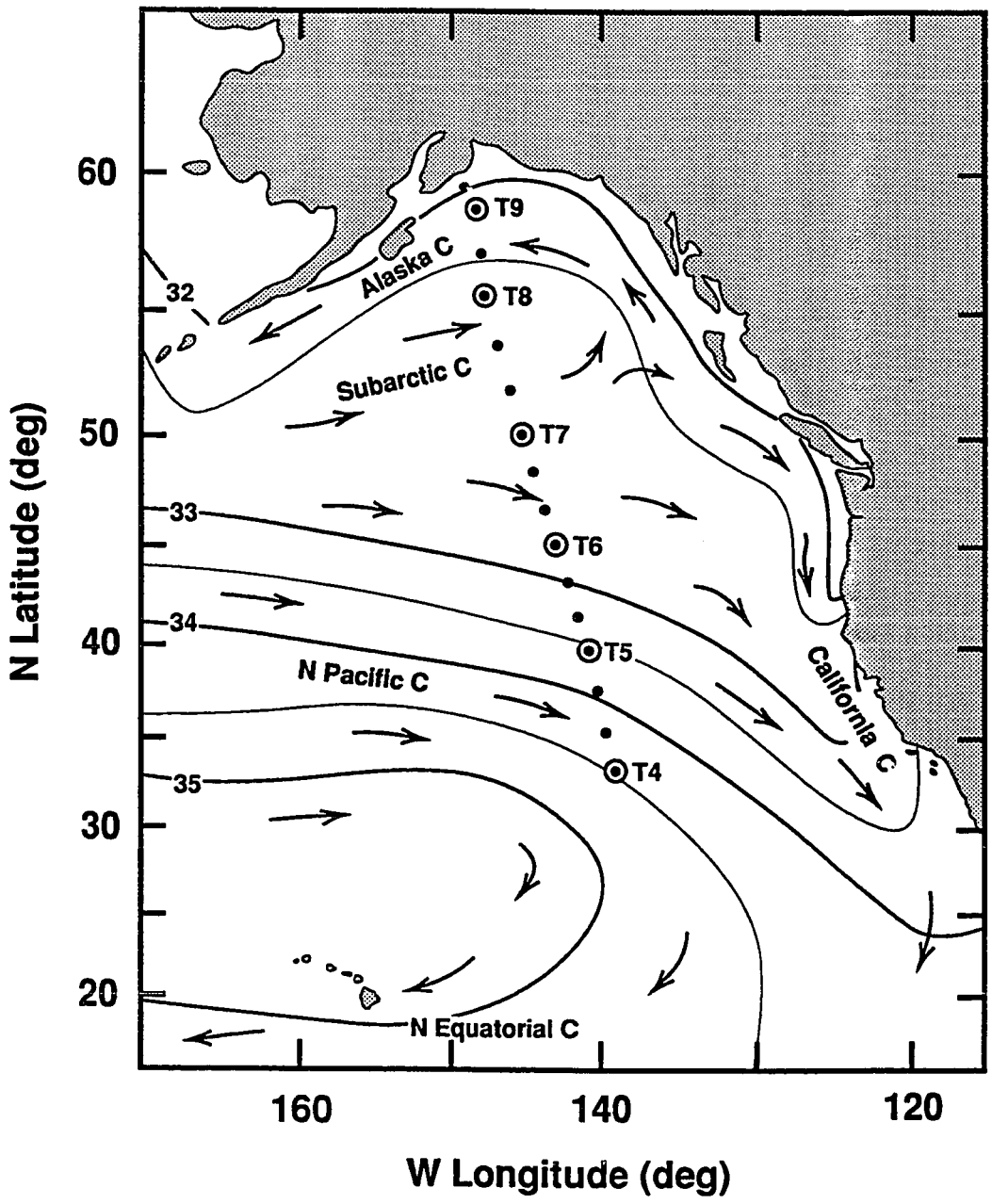

Figure 1. VERTEX 7 station positions and oceanographic features (adapted from Martin *et al.*, 1989). Station locations are listed in Table 1. Trace metal stations are T4-T9, and salinity isopleths are in PSU.

Table 1. VERTEX 7 CTDO station positions and dates. "T" indicates trace metal sampling stations. Type of fluorescence obtained during the cast is denoted by CF for chlorophyll fluorescence and PF for phycoerythrin fluorescence.

Station	North Latitude (deg min)	West Longitude (deg min)	Fluoro Type	Date (GMT)	Time (GMT Local)
1, T4	33 00.4	139 00.2	CF	26 Jul 87	0043 1527
1, T4	32 59.8	139 00.3	PF	26 Jul 87	1510 0554
2	35 12.4	139 35.2	PF	28 Jul 87	0028 1510
3	37 25.1	140 10.7	CF	28 Jul 87	1541 0620
4, T5	39 35.8	140 45.7	CF	29 Jul 87	0655 2132
4, T5	39 35.6	140 43.6	PF	29 Jul 87	2118 1155
5	41 23.8	141 28.9	PF	01 Aug 87	0120 1554
6	43 11.9	142 10.4	CF	01 Aug 87	1421 0452
7, T6	44 59.8	142 52.2	CF	02 Aug 87	0258 1727
7, T6	44 59.9	142 53.4	PF	04 Aug 87	0146 1614
8	46 40.3	143 32.9	PF	04 Aug 87	1336 0402
9	48 20.7	144 16.4	CF	05 Aug 87	0205 1628
10, T7	49 59.7	145 00.1	CF	05 Aug 87	1418 0438
10, T7	50 01.6	144 59.5	PF	07 Aug 87	0232 1652
11	51 49.8	145 49.7	PF	09 Aug 87	0521 1938
12	53 39.7	146 41.4	CF	09 Aug 87	1810 0823
13, T8	55 30.1	147 30.5	CF	10 Aug 87	0655 2105
13, T8	55 29.3	147 22.1	PF	12 Aug 87	0812 2223
14	57 07.8	147 44.7	PF	13 Aug 87	0328 1737
15, T9	58 41.5	147 56.6	PF	13 Aug 87	1457 0505
15, T9	58 40.9	147 57.2	CF	13 Aug 87	2335 1343
16	59 23.5	148 53.2	CF	14 Aug 87	0605 2009

Table 2. Algorithms and regression coefficients used to convert raw CTDO data. Primed variables (e.g. S′) represent raw data. The oxygen algorithm is discussed in Appendix 1.

Salinity (PSU) =>	$S = S' + a + bT$
Temperature (C) =>	$T = a + bT'$
Pressure (dbar) =>	$P = P' + a + bT_p + cT_p^2$
% Transmission (m^{-1}) =>	$\%T = a + b\%T'$
Rescaled Fluorescence (FU) =>	$ReF = {}_{10}(a + bF')$
Dissolved Oxygen (ml l^{-1}) =>	$O_2 = (a+bIO_2)O_2' * \exp(c(T + d(T_o) + eP)$

		a	b	c	d	e	N	Sy	r
S	(PSU)	-0.346	0.0337				95	0.037	0.962
T	(C)	-1.147	0.986				129	0.103	1.000
P	(dbar)	10.46	-0.0183	4.79e-6			14	0.136	0.999
O_2	(ml l^{-1})	-0.05	2.04e-3	-0.0234	1	4.22e-4	127		
%T	(m^{-1})	83.3	-0.0096				7	0.493	-0.195
ReF_{685}	(FU)	-4.682	0.0678				37	0.426	0.911
ReF_{590}	(FU)	-2.341	0.0678				0		

Temperature was corrected by comparison to standard reversing thermometers. Post cruise calibrations obtained with a dead weight pressure stand were applied to pressure transducer data. Since it has become common practice to use corrected pressure as the vertical independent variable and because pressure in decibars (dbar) is numerically equivalent to depth in meters (m), the terms "pressure" and "depth" are used synonymously.

The Beckman oxygen electrode (Greene *et al.*, 1970) was modified by placing a thermistor within 1 mm of the membrane. Thus, the oxygen reduction current as well as the membrane temperature were individually measured. Dissolved oxygen calibration samples were analyzed during the cruise using the Carpenter modification (1965) of the Winkler titration method, and oxygen profiles were corrected according to the algorithm developed by Owens and Millard (1985, Appendix 1).

The total attenuation coefficient was measured in the blue (Wratten 45, 480 nm) with a modified transmissometer based on the Scripps Institute of Oceanography Visibility Laboratory design (Austin and Petzold, 1977). The transmissometer projects a cylindrically limited light beam from a low current halogen lamp through a 1 m folded pathlength. A silicon photodiode detects that fraction of light not attenuated by absorption or scattering via water molecules, particulates, and dissolved materials.

Transmissometer gain setting and instrumental drift over time must be considered when interpreting total attenuation distributions. Air calibration readings obtained just prior to CTDO casts were used to account for these two sources of error. The theoretical air to water transmittance ratio due to Fresnel reflectance for a transmissometer with four glass/medium interfaces is 85.5% (Austin and Petzold, 1977). Since it is impractical to adjust the gain of the transmissometer so that the theoretical air calibration value is obtained before each CTDO cast, the ratio of 85.5% to field air calibrations was applied to the profiles.

The theoretical to field air calibration ratio may be applied in two ways: as a single ratio of 85.5% to the mean of all field air calibrations or as a sequence of ratios based upon individual air calibrations. The latter method is applicable when instrumental drift over the duration of a cruise has occurred. Although the correlation for air calibration readings versus time was not significant (Fig. 2), instrumental drift was corrected because sample size was small (n=7). This correction also ensured that any apparent trend in particle concentration through the section would not be an instrument artifact. Thus, the regression obtained from air calibration readings versus time was used to determine the theoretical to field calibration ratio for each station.

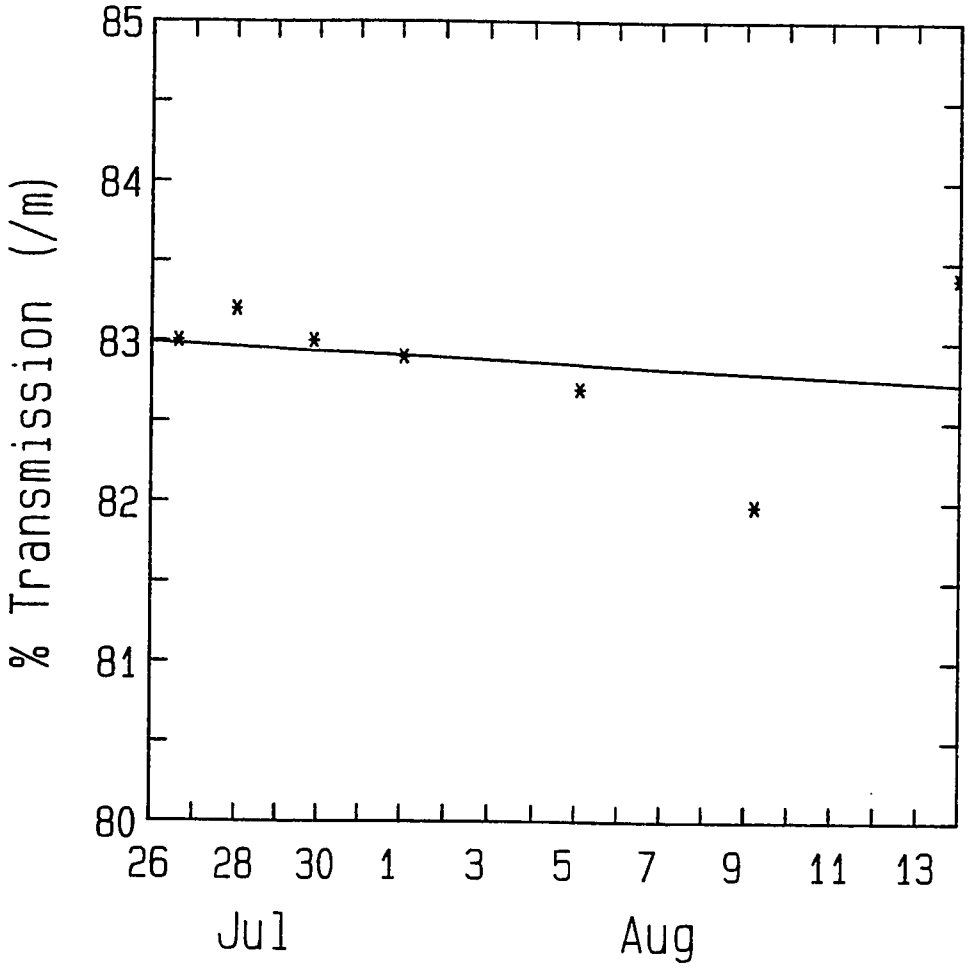

Intercept = 8.333e 01
Slope = -1.333e-02
R↑2 = 0.0386
Syx = 0.4927
N = 7

Figure 2. Correlation diagram for transmissometer drift over time.

In addition to instrument gain and drift errors, VERTEX 7 transmissometer data were also corrected for signal offsets apparently caused by a loose filament in the halogen lamp. The offsets occurred in two ways: intracast, where only a portion of a profile was affected, and intercast, where an entire profile was offset. Intracast shifts appeared either as sudden offsets (Fig. 3a) or as low frequency offsets (Fig. 3c). In cases where the offset was solitary (Fig. 3a), a ratio of the mean of the 20 preceding values to the mean of the 20 succeeding values from the offset was determined. The offset portion of the cast was corrected by multiplication with that ratio (Fig. 3b). Since the portions of profiles containing low frequency offsets (Fig. 3c) were not long enough for time series analysis, these data were manually corrected by eye (Fig. 3d).

Intercast offsets were detected by dividing transmissometer profiles into 100 m bins and calculating the mean value for each bin. Comparison of the deepest bin (1900-2000 m) values showed that intercast shifts occurred at 33.0°, 37.4°, 39.6°, and 50° N (Fig. 4a). Since 33.0°, 39.6°, and 50° N included trace metal sampling, each of these offset profiles were one of a pair of transmissometer profiles. The ratio of the overall mean value at depth (1500-2000 m) for the unshifted to the shifted profiles was used as the correction multiplier.

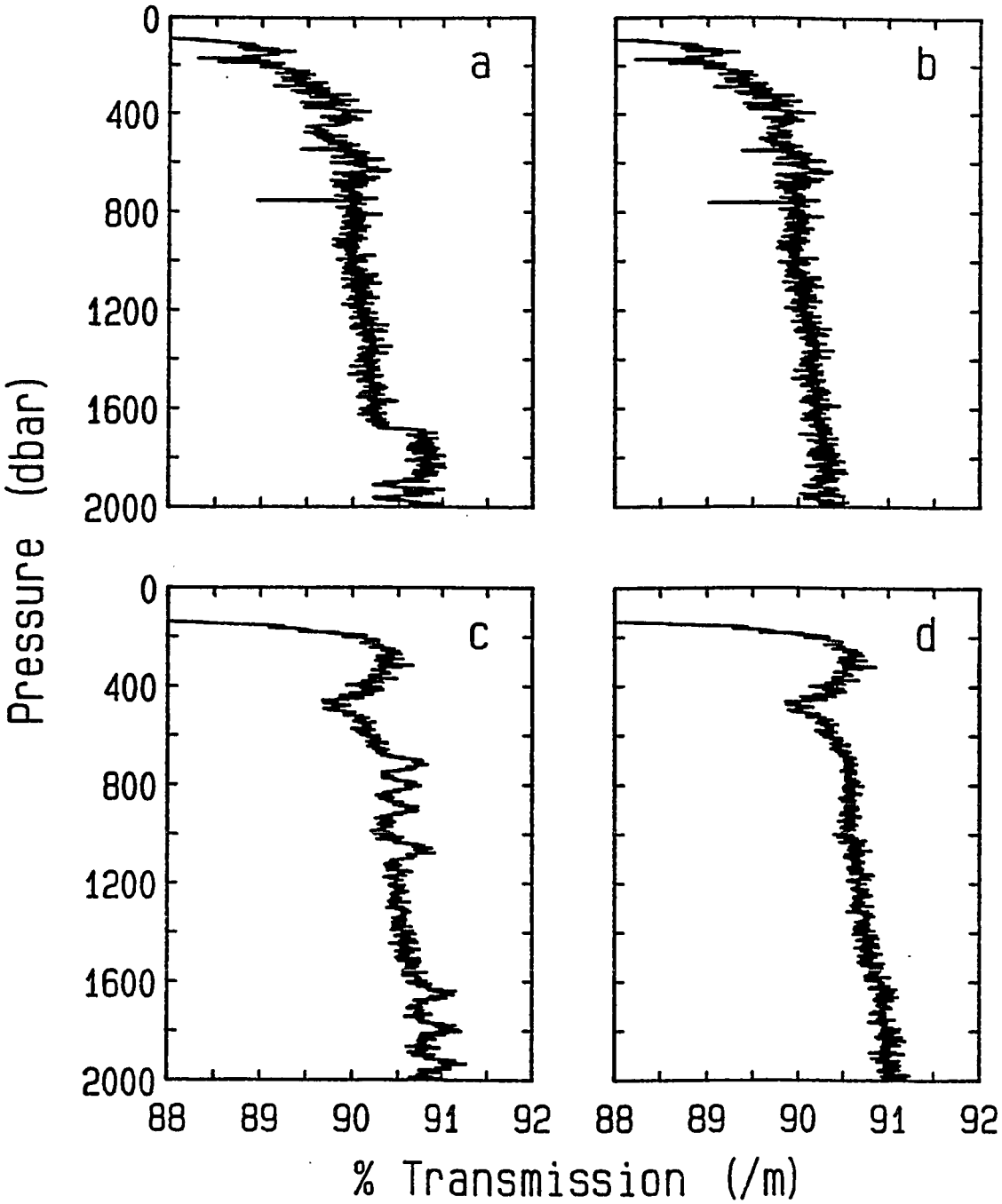

Figure 3. Before and after intracast corrections for transmissometer profiles. a) Profile at 37.4° N showing a sudden offset near 1700 m. b) Corrected profile at 37.4° N. c) Profile at 33.0° N showing low frequency offsets. d) Corrected profile at 33.0° N.

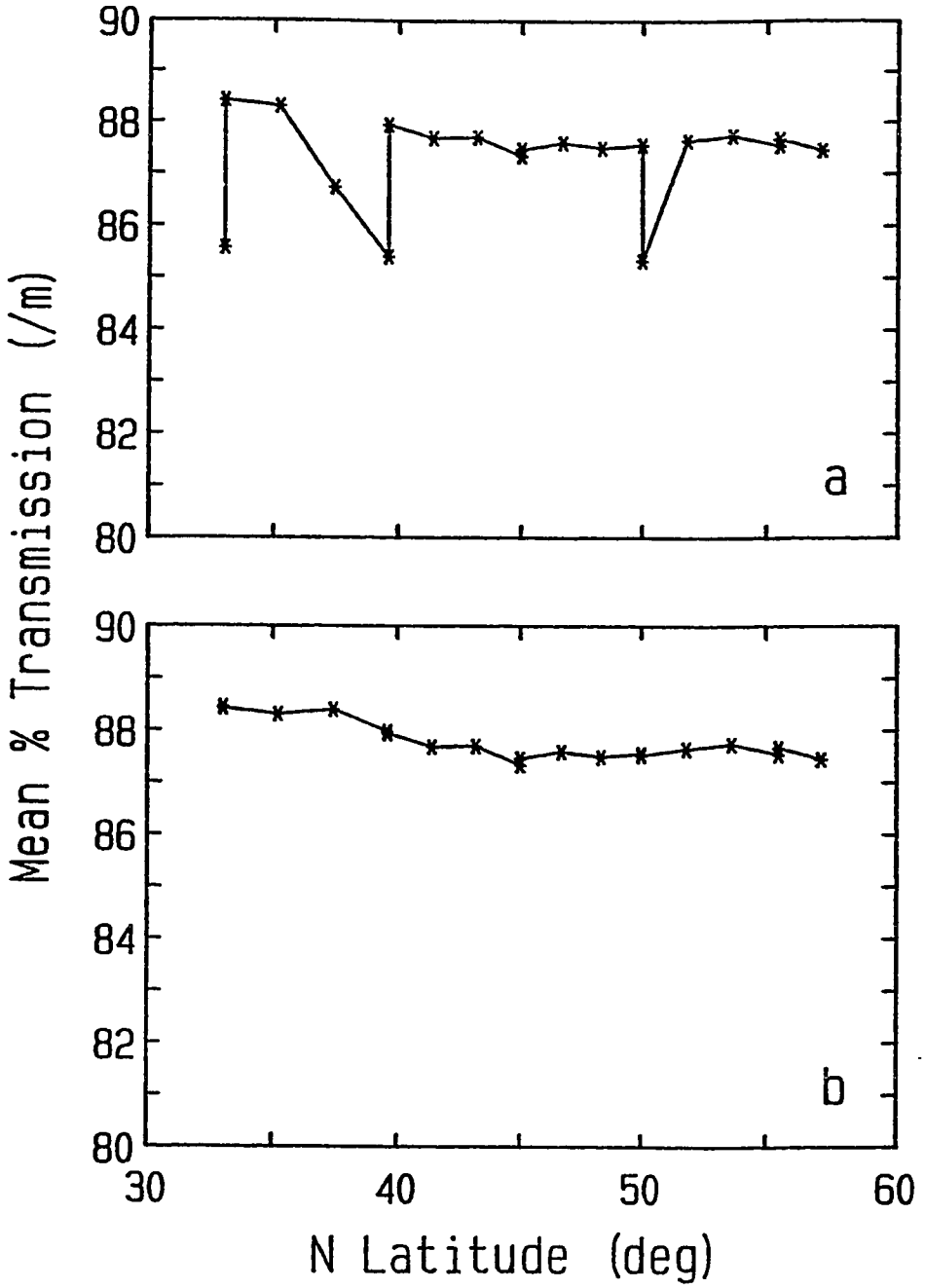

Figure 4. Before and after transmissometer intercast corrections. a) Mean % transmission values for 1900-2000 m show four intercast shifts at 33.0°, 37.4°, 39.6°, and 50° N. b) Mean % transmission values for 1900-2000 m after intercast shifts were corrected.

Data at 37.4° N were corrected by forming ratios with the means (1500-2000 m) from the preceding and the corrected succeeding casts. Thus, the profile at 37.4° N had two possible correction multipliers. Each of these ratios were individually applied to the binned cast data at 37.4° N. To select the best correction ratio, the "corrected" binned profile using the ratio obtained from the preceding cast was compared with the preceding binned cast data (i.e. binned data at 37.4° N were divided by the binned data at 35.2° N). This comparison was also done with the succeeding cast. Both profiles of ratios were plotted and compared (Fig. 5). The profile that came closest to a value of 1.00 at depth (1500-2000 m) was selected as the offset correction (Fig. 4b). Following VERTEX 7, transmissometer electronics were repaired and this is no longer a problem.

The *in situ* Variosens II fluorometer (Frungel and Koch, 1980) projects light (xenon flash lamp) through the surrounding water exciting pigment molecules into fluorescing while simultaneously sensing their emission with a silicon photodiode. Modifications to the pressure housing and to the thickness of the projector and receiver windows of the fluorometer are such that the water sampling volume is 10 ml. The Variosens II fluorometer is log-scaled over four decades; however, observations generally varied over three orders of magnitude.

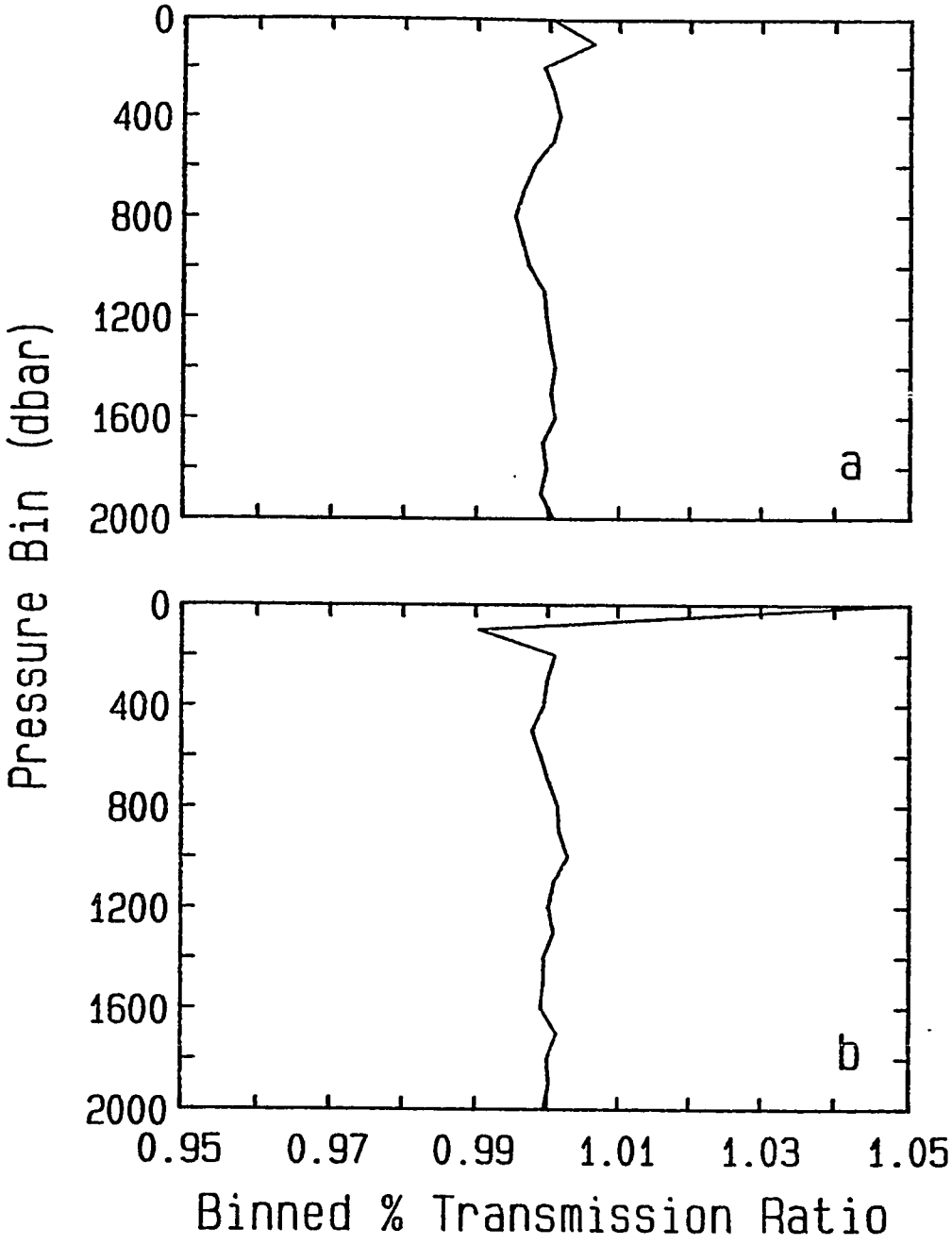

Figure 5. Binned % transmission ratio profiles used to determine the correction multiplier for the intercast shift at 37.4° N. a) Profile of binned data ratios between 35.2° and 37.4° N. b) Profile of binned data ratios between 37.4° and 39.6° N. Ratios at depth (1500-2000 m) least fluctuated about 1.00 between 37.4° and 39.6° N.

During VERTEX 7, observations for phycoerythrin and chlorophyll fluorescence were obtained through the use of a broad band blue excitation filter (Balzer, 336-571 nm), a 20 nm band pass emission filter with peak spectral transmissivity in the yellow/orange (Ditric, 580-600 nm) for phycoerythrin, and a high pass emission filter in the red (Corning 2-64, 667 nm half-power) for chlorophyll (Fig. 6). Phycoerythrin and chlorophyll fluorescence profiles were obtained alternately from station to station by exchanging the emission filters between each CTDO cast; however, since at least two casts were made at trace metal stations, both types of fluorescence profiles were acquired at these locations (Table 1).

Chlorophyll *a* samples were filtered through Whatman GF/F (0.7 μm) glass fiber filters and frozen for analysis ashore. Pigments were extracted in 90% acetone, and chlorophyll *a* concentrations were determined by fluorometric analysis (Yentsch and Menzel, 1963; Holm-Hansen, 1965) with a G. K. Turner III fluorometer. Although converted chlorophyll fluorescence is based upon chlorophyll *a* concentrations (Fig. 7), it is reported as "rescaled fluorescence" (ReF_{685}) to acknowledge that chlorophyll *a* fluorescence quantum yields are variable (Falkowski and Kiefer, 1985). The means for phycoerythrin analysis were not available at Moss Landing Marine Laboratories during VERTEX 7; therefore, phycoerythrin

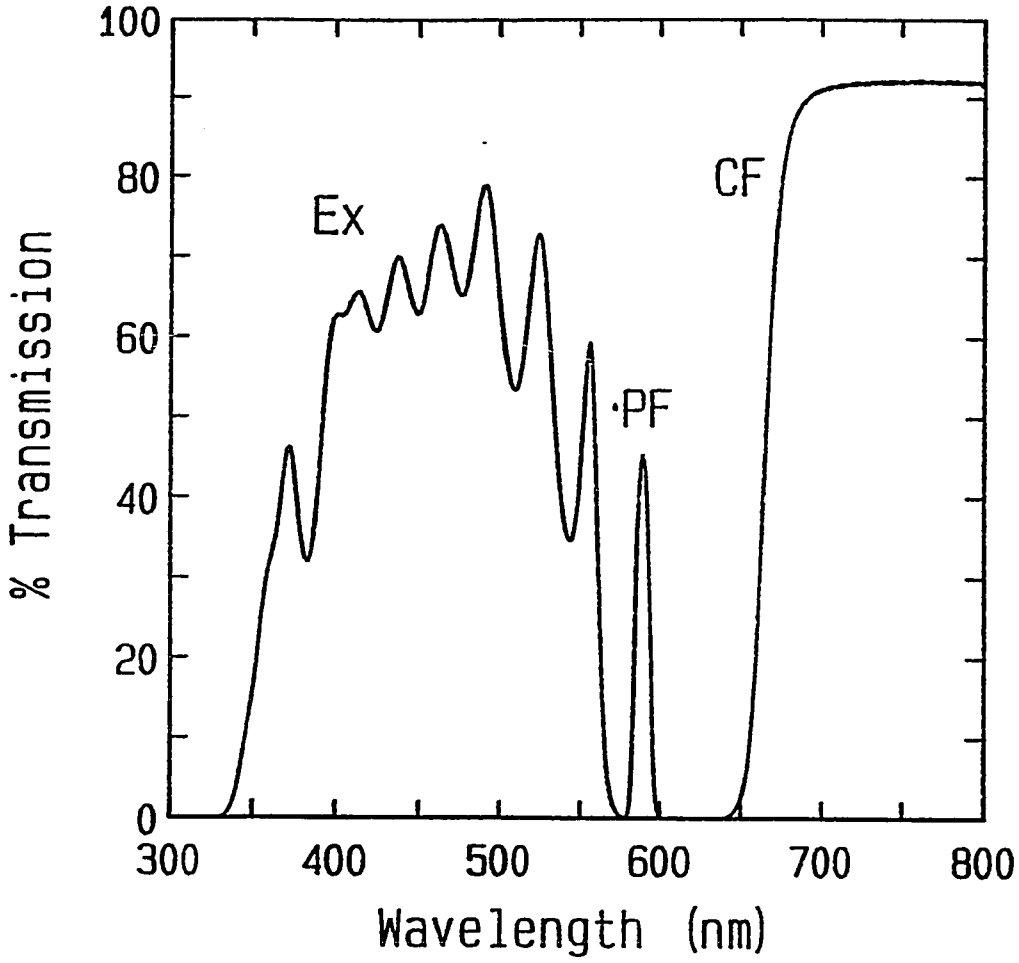

Figure 6. Transmissivity of the fluorometer filters used during VERTEX 7. Individual filters are Ex for broad band blue excitation (336-571 nm), PF for phycoerythrin fluorescence (580-600 nm), and CF for chlorophyll fluorescence (667 nm half-power).

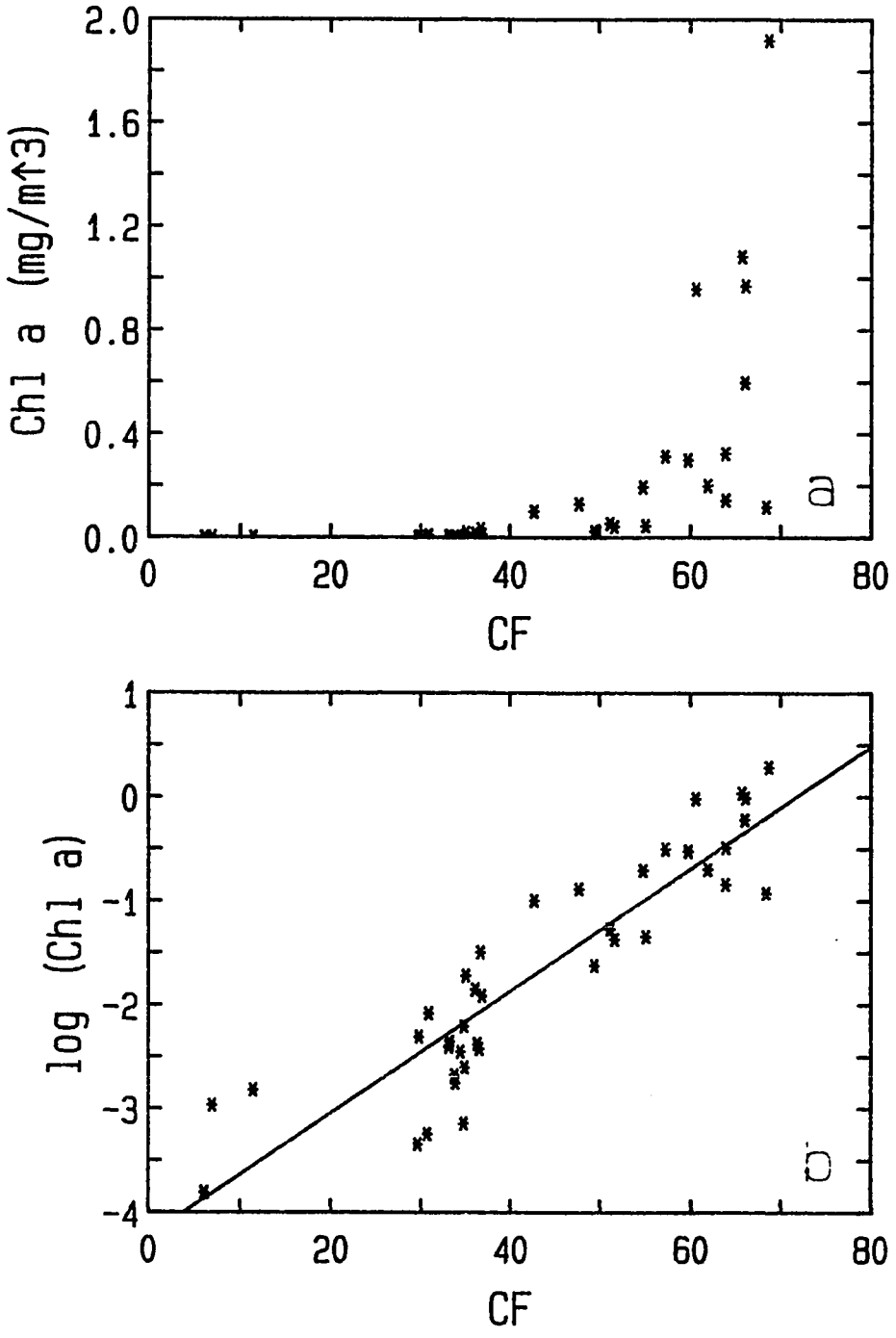

Figure 7. Comparison of chlorophyll a calibration samples versus chlorophyll fluorescence (a). Log-scale effect removed allows for linear regression and and conversion of chlorophyll fluorescence to rescaled fluorescence.

pigment calibration samples were not obtained. Phycoerythrin fluorescence values, however, were linearized (ReF_{590}) by using half the offset and the same slope used for chlorophyll fluorescence (Table 2). Use of the full chlorophyll fluorescence offset essentially reduced all ReF_{590} values to 0.00. Since chlorophyll and phycoerythrin fluorescence profiles at major "T" stations were obtained on separate casts hours apart (Table 1), raw fluorescence values (i.e. log-scaled) were interpolated against temperature to 0.1° C intervals before intercomparison between the bio-optical distributions.

RESULTS

Distributions of bio-optical properties are dependent upon physical as well as biological processes. An understanding of the physical processes is especially important when data are collected over a wide geographic area where water mass characteristics change dramatically. Lateral distributions of salinity and temperature (Figs. 8-9) best illustrate the local hydrography of the Northeast Pacific during VERTEX 7.

The southern portion (33° to 41° N) of the cruise track crossed the North Pacific frontal system, which is best shown by the salinity distribution (Fig. 8) where sharp surface gradients were observed. The location of the Northern Subtropical Front (Lynn, 1986; Roden, 1980), which appears near the northern edge of the subtropic front, is indicated by a salinity gradient centered at 34° N, and the position of the subarctic front is shown by another salinity gradient from 38° to 41° N. Corresponding gradients in potential temperature (theta) and potential density anomaly (sigma-theta) were absent; instead, the isopleths for both fields (Figs. 9-10) gently and continuously shoaled throughout the frontal region. This is indicative of a "density compensated" frontal system where changes in salinity are compensated by corresponding changes in temperature, leading to little or no change in density (Roden, 1980).

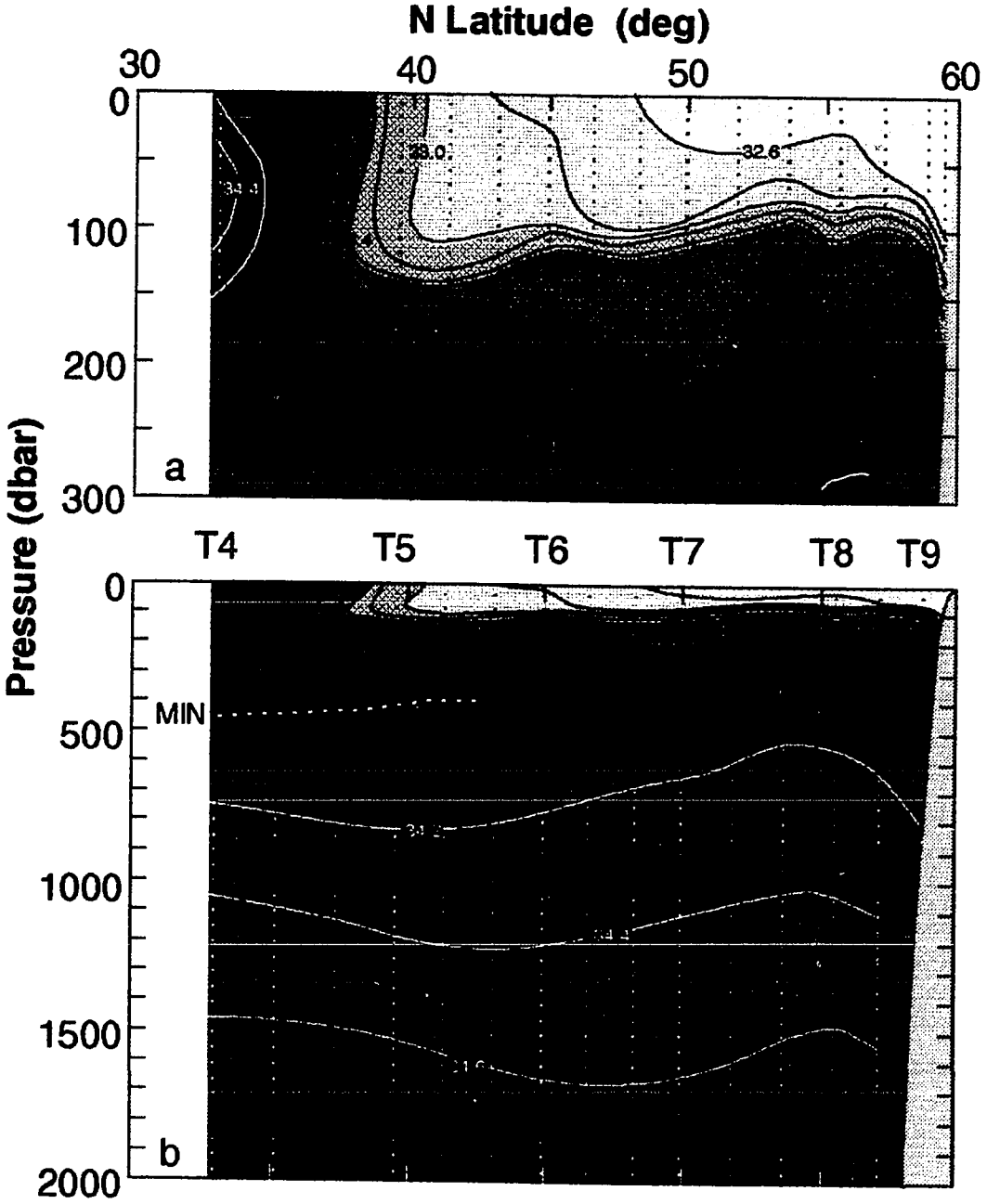

Figure 8. Lateral salinity (PSU) distribution for VERTEX 7. The Northern Subtropical Front is centered at 34° N and the subarctic front is located at 38° to 41° N. Dashed line shows depth of minimum in (b).

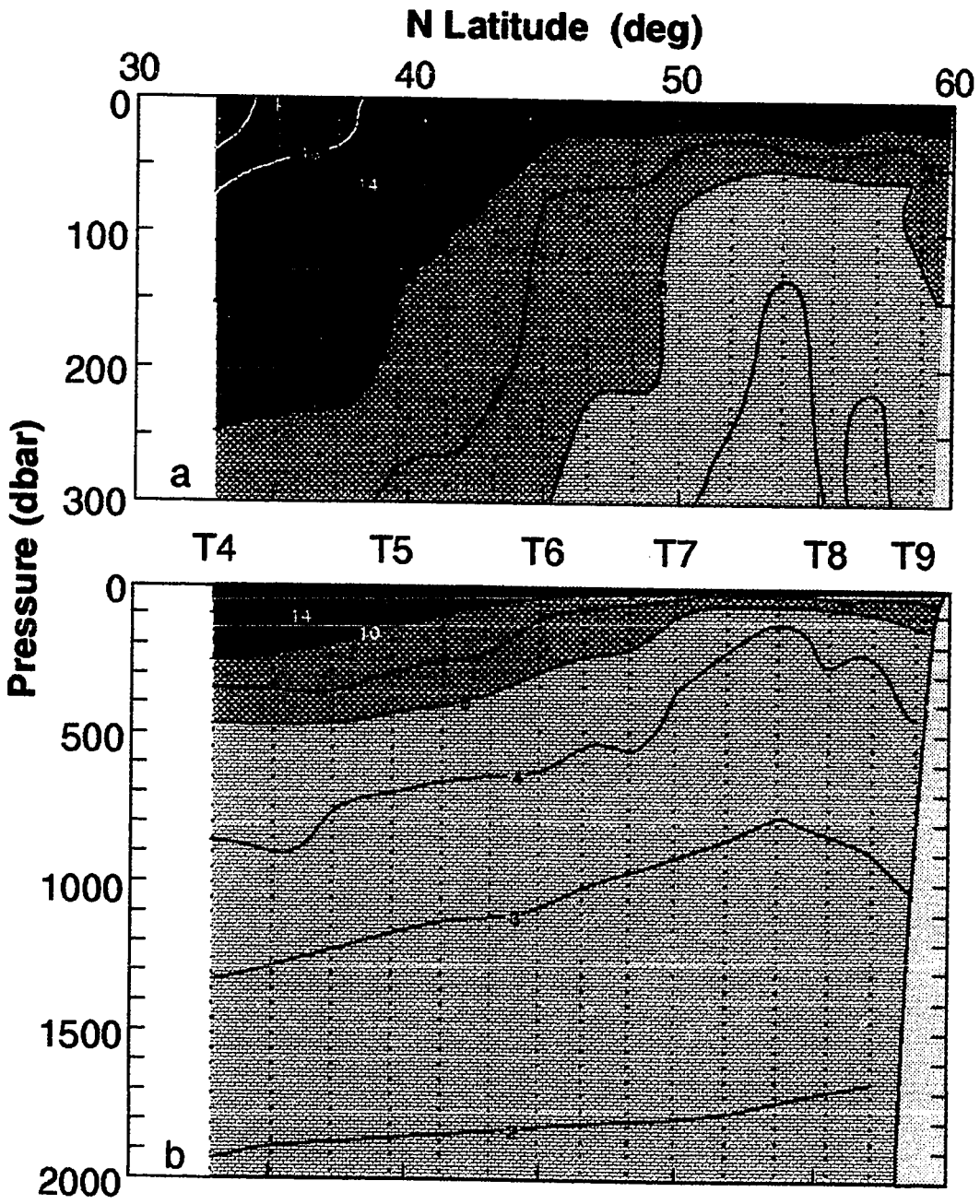

Figure 9. Lateral potential temperature (°C) distribution.

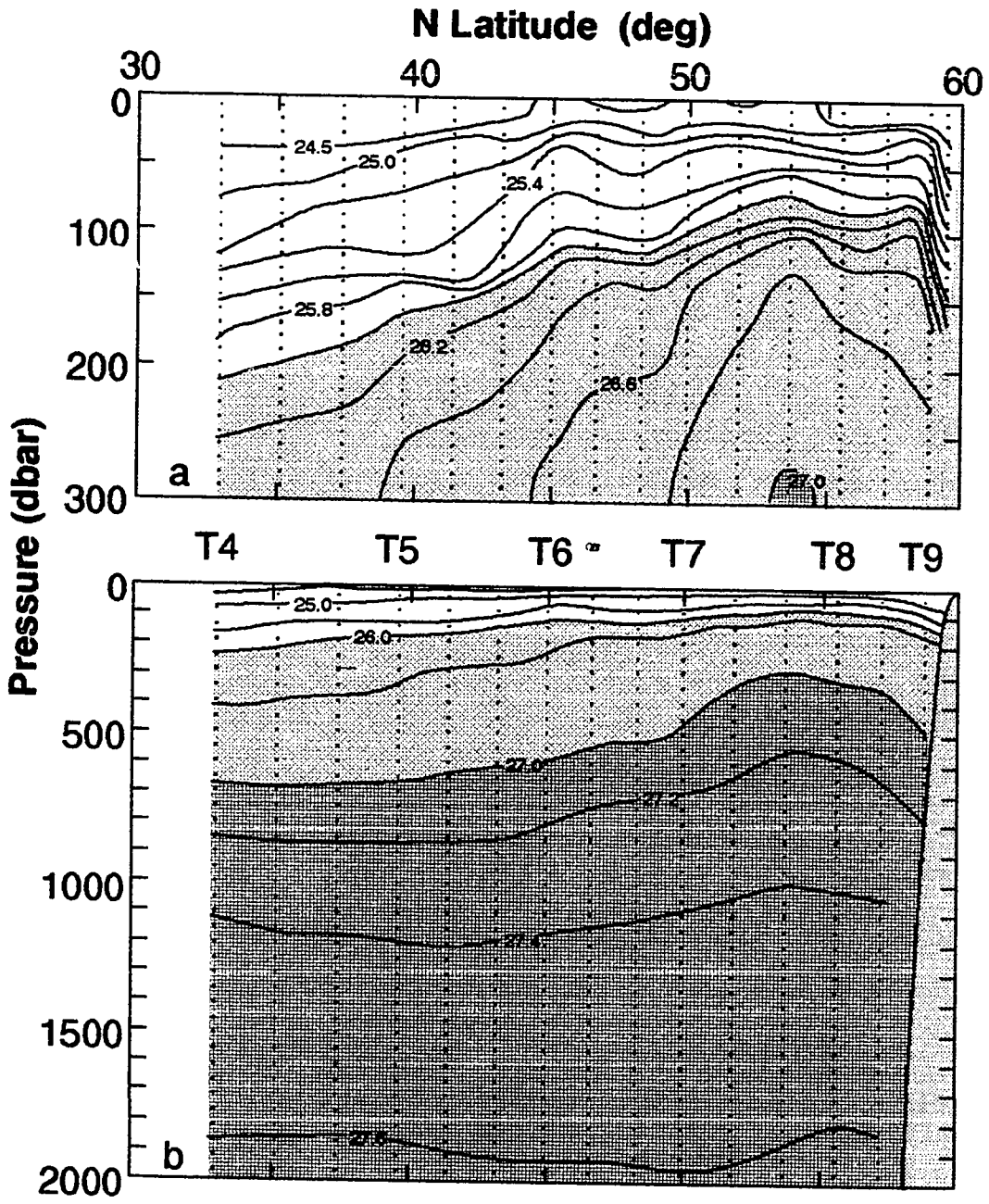

Figure 10. Potential density anomaly (sigma-theta) distribution.

North of the frontal system, circulation around the Alaska Gyre is reflected by a steeper incline in the subsurface isohalines, isotherms, and isopycnals (Figs. 8-10). The increased shoaling of the isopleths between the subarctic front and 54° N represent the eastward flowing North Pacific Current. The isopleths peak near 54° N, indicating the position of the Alaskan Dome (Bennett, 1959), before deepening to the north as the westward flowing portion of the Alaska Current (Favorite *et al.*, 1976).

The steep vertical salinity gradient (32.6-33.8 PSU) from the surface to 200 m in the Gulf of Alaska (Fig. 8) is due to coastal fresh water discharge. This subarctic salinity distribution in the Northeast Pacific is important locally in the Gulf of Alaska as well as on an oceanic scale in the North Pacific. In the Gulf of Alaska, the shallow vertical salinity gradient (Fig. 8) is large relative to the temperature gradient (Fig. 9), thus the resulting baroclinic flow is predominantly controlled by the salinity distribution. On a larger scale, this low salinity surface water effectively prevents bottom water formation in the North Pacific, and is important in the formation of Pacific Intermediate Water (Reid, 1973).

The T-S plot (Fig. 11) for the transect further illustrates the importance of the salinity distribution in the subarctic North Pacific. The main pycnocline south of the frontal system is due to the vertical temperature

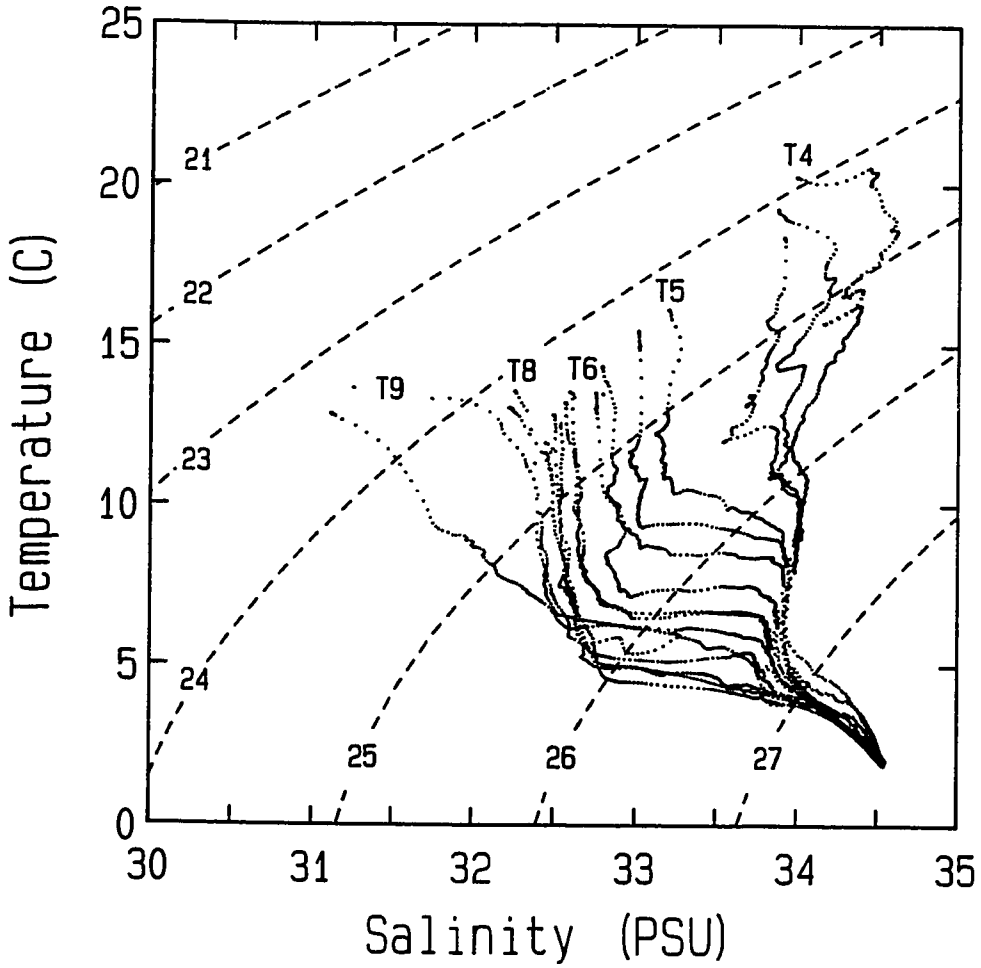

Figure 11. T-S relationship for VERTEX 7. Dashed lines show sigma-t (σ_t) surfaces. Stations south of the Pacific subarctic front (~T5) are thermally stratified, while those north of the front are thermally stratified to σ_t~25.5-26.0 and salinity stratified below this surface.

gradient while north of the subarctic front, it consists of a thermocline underlain by a halocline. This two component pycnocline leads to two corresponding hydrostatic stability layers (Fig. 12) in the upper 200 m. The shallower layer centered at 45 m at 33° N shoaled to 15 m at 59° N. The deeper layer shoaled more steeply from 190 to 100 m over the same latitudinal range.

Lateral distributions of dissolved oxygen (O_2), total attenuation coefficient (c), chlorophyll fluorescence (CF), and phycoerythrin fluorescence (PF) show near-surface (primary) maxima as well as intermediate depth (tertiary) pigment maxima (Figs. 13-16). South of the Alaskan Dome, the subsurface maxima were located between the hydrostatic stability layers; however, north of the Dome, they were coincident with the shallower stability layer. Both c and PF values (Figs. 14, 16) increased and shoaled from 100 m at 33° N to the surface near the Alaskan Dome. The c maximum briefly surfaced north of the Dome between 55.5° and 57° N. The PF maximum surfaced south of the Dome at 52° N and remained there through to 58° N. In contrast, O_2 and CF (Figs. 13, 15) maxima shoaled from 80 and 140 m, respectively, through the frontal system then leveled off near 30 m. While the O_2 maximum remained at this depth to the northern extent of the transect, CF further shoaled to 10 m north of the Alaskan Dome.

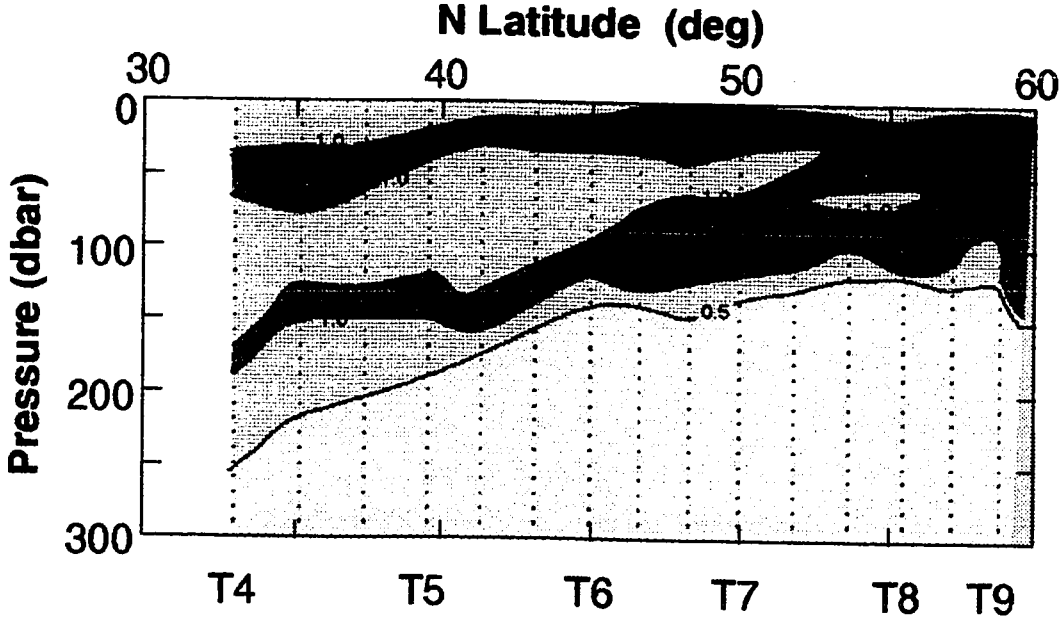

Figure 12. Lateral distribution of hydrostatic stability (10^{-5} m^{-1}). The shallower stability layer is due to the thermocline and the deeper layer corresponds with the underlying halocline.

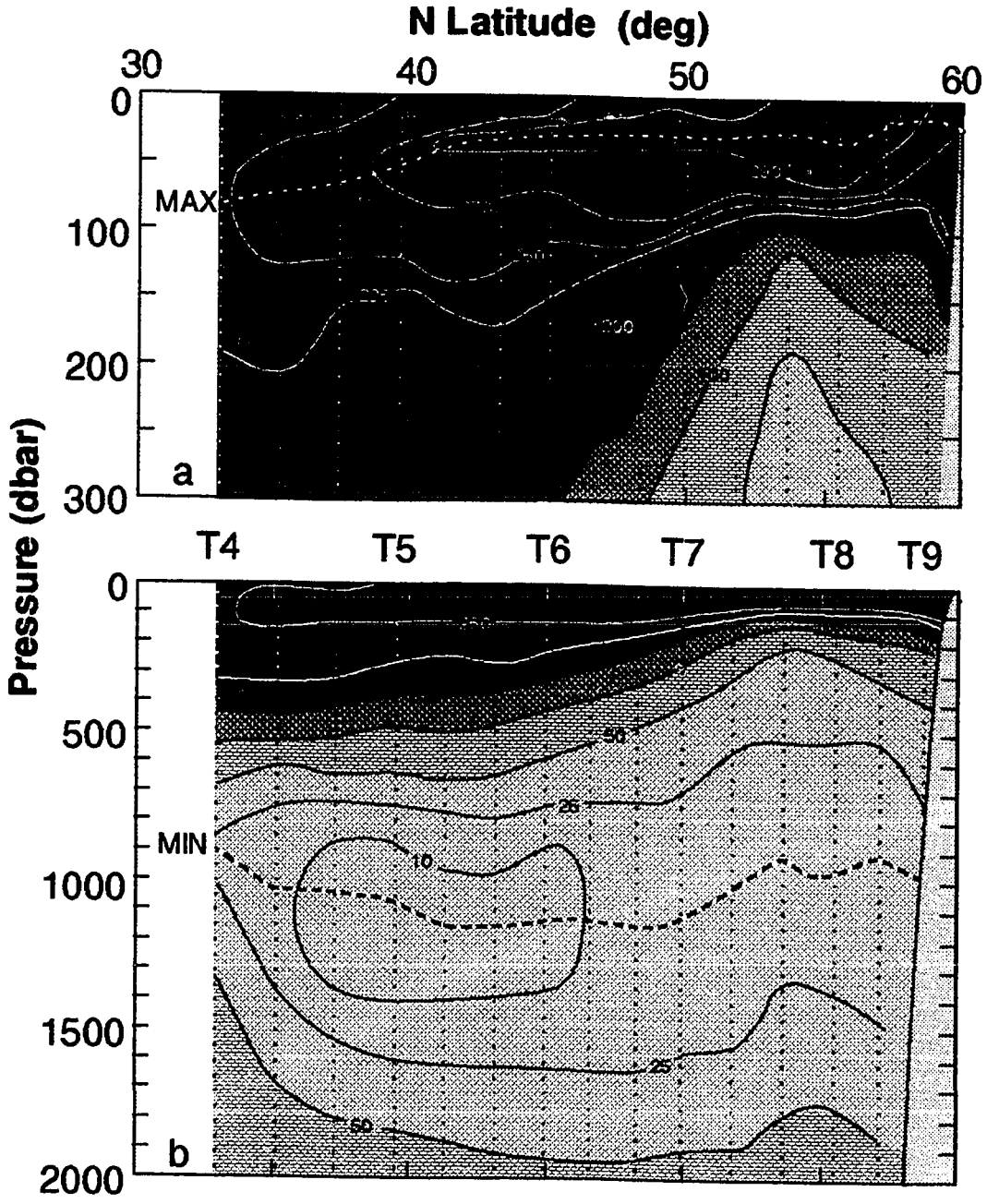

Figure 13. Dissolved oxygen (μmoles kg^{-1}) distribution. Dashed lines indicate the depth of the maximum in (a) and of the minimum in (b).

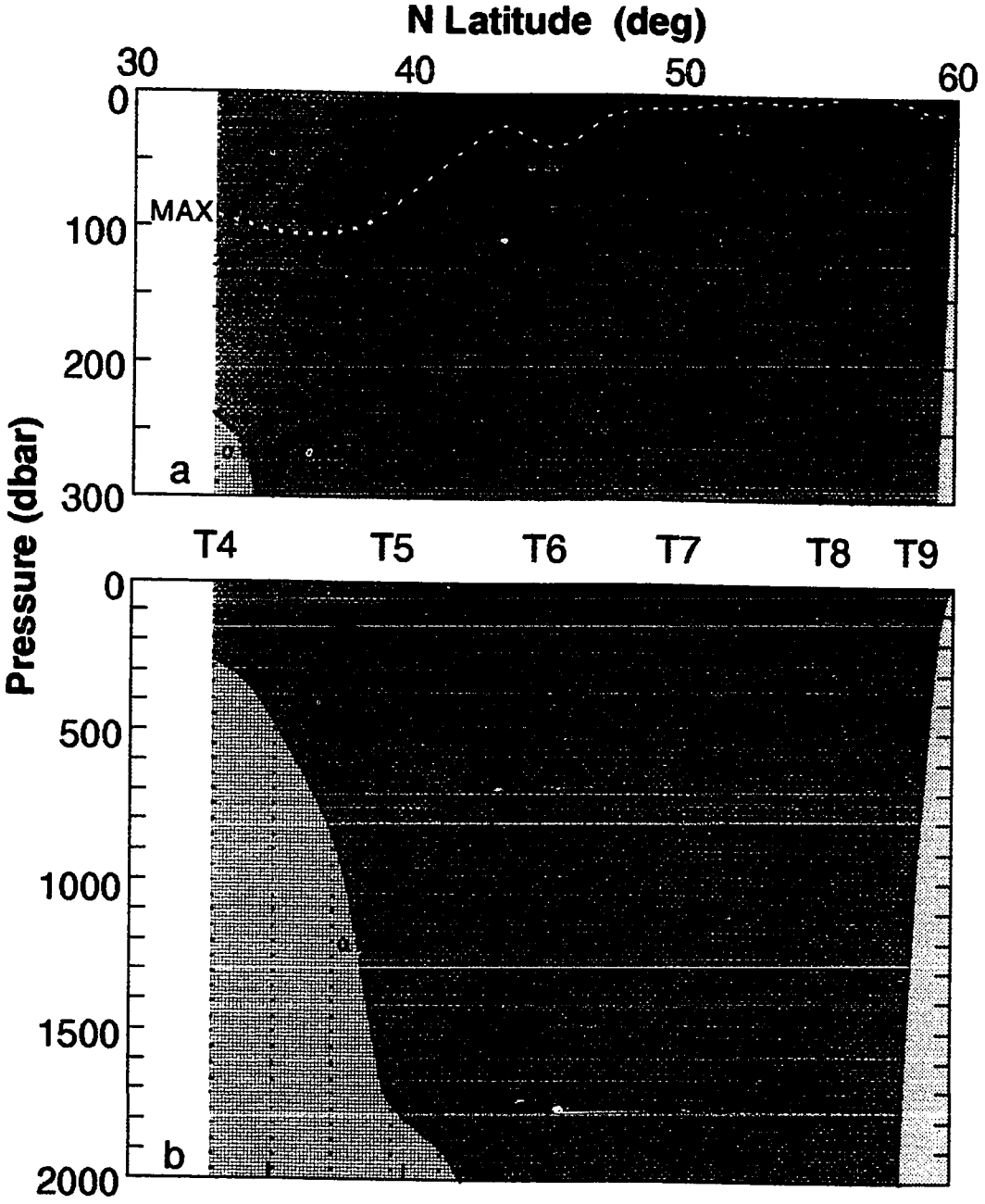

Figure 14. Total attenuation coefficient, c (m^{-1}), measured at 480 nm. Dashed line indicates depth of subsurface maximum in (a).

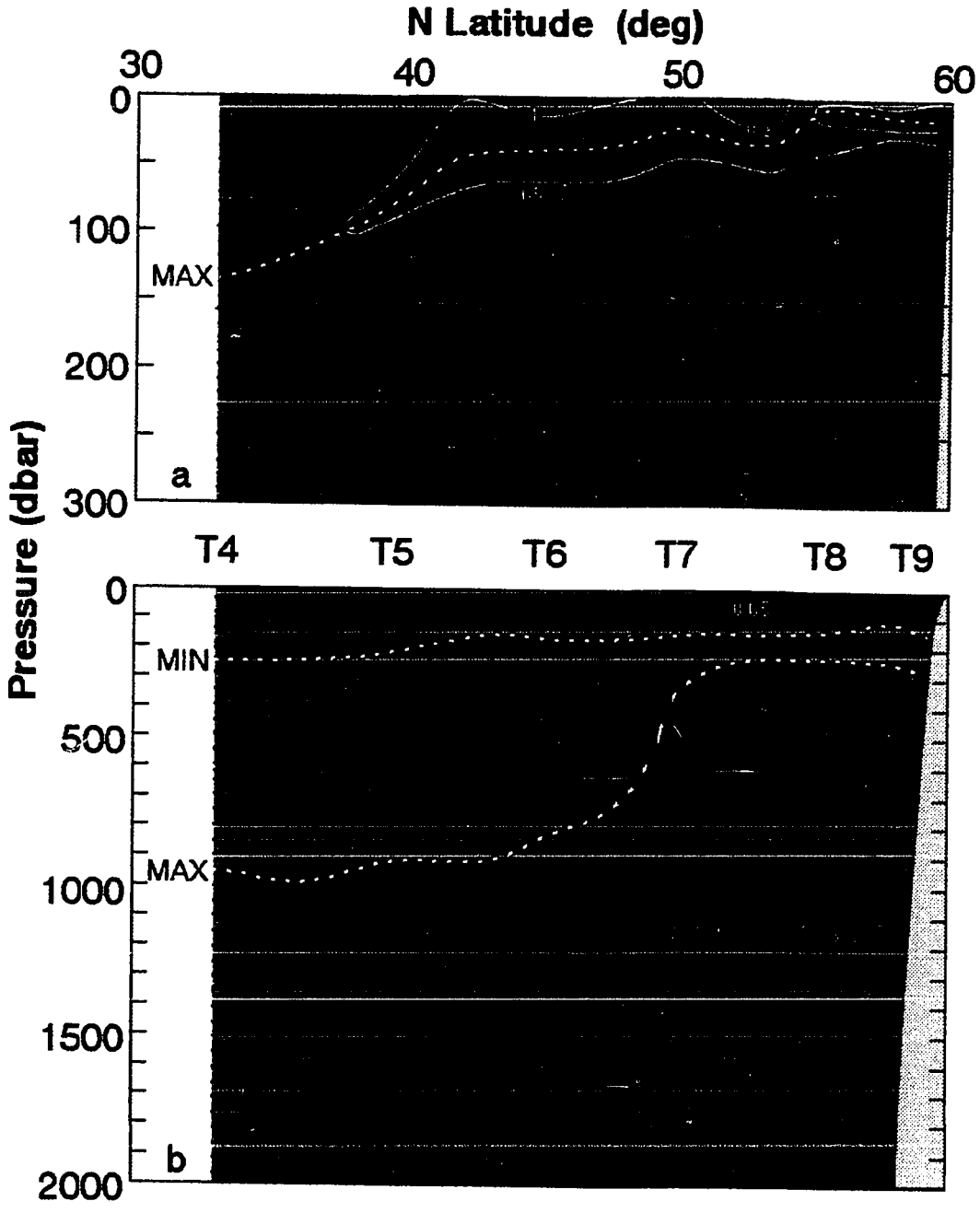

Figure 15. Chlorophyll fluorescence (685 nm) distribution. Note that values are rescaled (i.e. arithmetic). Dashed lines indicate depths of the maximum in (a) and of the minimum and maximum in (b).

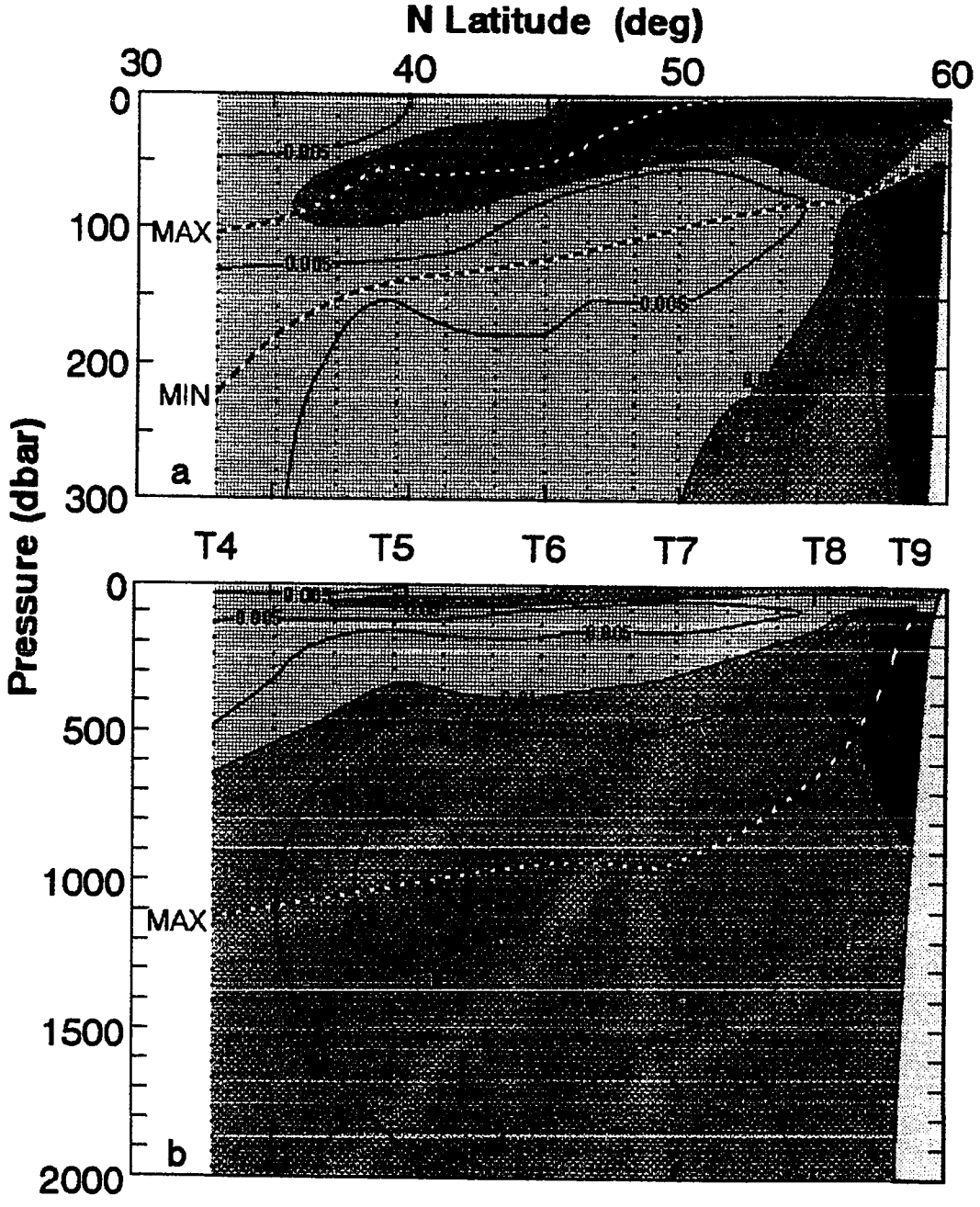

Figure 16. Phycoerythrin fluorescence (590 nm) distribution. Note that values are rescaled (i.e. arithmetic). Dashed lines show depths of the primary maximum and minimum in (a) and of the tertiary maximum in (b).

The minima separating the shallow and intermediate depth maxima for both pigments shoaled from south to north, and occurred beneath the deeper stability layer. The core of the CF minimum (Fig. 15) ranged from 250 m at 33° N to 150 m at 59° N. In contrast, shoaling of the PF minimum (Fig. 16) was more severe and the intensity of the minimum was nearly constant south of the Alaskan Dome. Through the frontal system, the PF minimum rose from 230 m to 140 m. North of the frontal system, the PF minimum shoaled to 50 m at 58° N.

Intermediate depth features were not nearly as well correlated as those in the near-surface waters. The core of the oxygen minimum (Fig. 13), near 1000 m for the entire transect, corresponded fairly closely with the 27.4 isopycnal (Fig. 10). Lowest oxygen values were found between 35° and 46° N. Maximum values in CF (Fig. 15) were located at 900 m south of 48° N. Between 48° and 51° N, the CF maximum shoaled very steeply to 250 m and remained at this depth to 59° N. PF maximum values (Fig. 16) gently shoaled from 1100 m at 33° N to 950 m at 50° N, then rapidly shoaled to 100 m at 58° N. Largest PF values at 1000 m were found at 38° to 42° N, coinciding with the area of lowest oxygen values.

DISCUSSION

The bio-optical distributions discussed here are significantly different from other recent studies (Pak *et al.*, 1988; Strass and Woods, 1988) because observations for both chlorophyll and phycoerythrin fluorescence as well as total attenuation extend to 2000 m. VERTEX 7 observations showed prominent near-surface fluorescence and particle maxima in subarctic waters, an underlying fluorescence minimum, and a fluorescence maximum at intermediate depths. This discussion will present hypotheses to account for these observed distributions and will focus on the interrelationships of these properties.

Total Attenuation

The total attenuation coefficient (c) accounts for absorption and scattering effects due to particles, dissolved material, and water molecules. VERTEX 7 attenuation data differ from others reported (Bishop, 1986; Pak *et al.*, 1988; Spinrad *et al.*, 1989) because they were measured in the blue (480 nm) through a 1 m transmissometer pathlength instead of in the red (665 nm) through 0.25 m.

Although Morel and Prieur (1977) showed that water absorption is much stronger in the red than in the blue, pure water c is 0.021 m^{-1} at 480 nm and 0.420 m^{-1} at 665 nm (Morel and Prieur, 1977), measurement of c in the red (c_{665}) has been favored in the past because gelbstoff (dissolved

humic substances) absorbance is minimal at longer wavelengths (Jerlov, 1976). Instrument stability is also improved since LED sources are stable and silicon diode detectors are more sensitive to red than to blue wavelengths (Bartz *et al.*, 1978). Gelbstoff in seawater is, however, closely linked with coastal areas where freshwater drainage is high (Jerlov, 1976), and Hoejerslev (1980) has concluded that degradation of plankton and detritus does not appreciably contribute to gelbstoff production in the open ocean. Thus, open ocean c measured in the blue (c_{480}) is due to minimal water absorption, particle scattering and absorption, and negligible gelbstoff absorption while c_{665} is due to maximal water absorption, particulate scattering and absorption, and minimal gelbstoff absorption.

Quantitative comparison of suspended particulate matter (SPM) versus total attenuation ratios between blue and red transmissometers shows a good correlation between VERTEX 7 data and those of other recent studies. The VERTEX 7 SPM:c ratio (Fig. 17) is 850 μg m l^{-1} while those of Pak *et al.* (1988) and Spinrad *et al.* (1989) are approximately 1280 μg m l^{-1} and 1230 μg m l^{-1}, respectively. The slopes from both data sets are estimated without differentiating between particle sizes. Bishop's (1986) open ocean (warm core ring) data give an SPM:c ratio of 1150 μg m l^{-1}. Thus, the relative sensitivity of VERTEX 7 data to Pak's is 1.51, to Spinrad's is 1.45, and to Bishop's

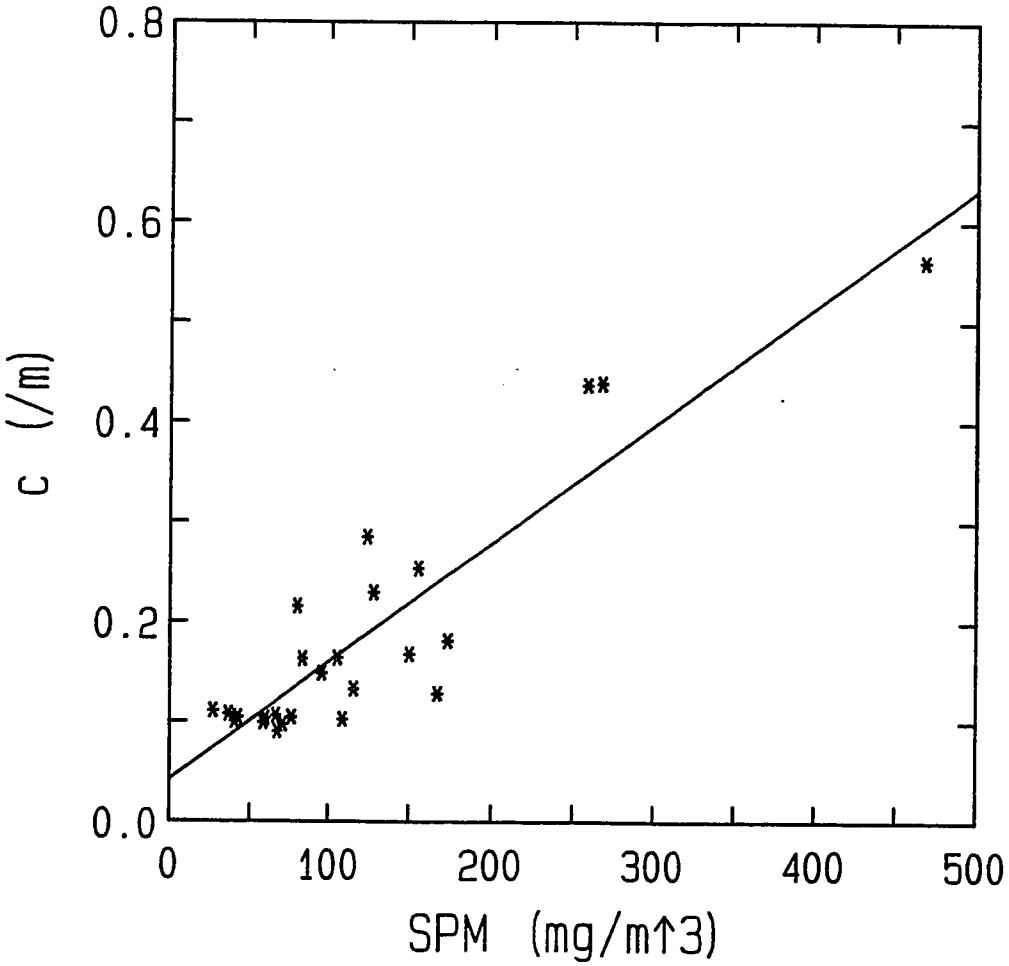

Figure 17. Total attenuation coefficient, c (m^{-1}), measured at 480 nm versus suspended particulate matter (SPM). Line indicates an SPM:c ratio of 850 μg m l^{-1}.

is 1.35. In other words, measurements of total attenuation at 480 nm are apparently 40% more sensitive to changes in attenuation than are measurements at 665 nm. These sensitivity ratios are remarkably close to the particle scattering wavelength dependence suggested by Morel (1973):

$$\left[\frac{480}{665} \right]^{-1.2} = 1.48 \qquad (1)$$

This strong agreement indicates that in oligotrophic waters, total attenuation is primarily due to particles, and that gelbstoff absorption is not important.

Fluorescence

Fluorescence (F), the "immediate" reemission of absorbed light energy, is a wavelength specific process. The emission wavelengths are longer than those absorbed, and in some instances, the absorption and emission wavelengths may overlap. This overlap is not desirable, and it should be noted that VERTEX 7 phycoerythrin fluorescence (PF) observations were not centered on the optimal wavelength of about 580 nm (MacColl and Guard-Friar, 1987) because of the broad band excitation filter (Fig. 6) used. When interpreting *in situ* fluorescence observations, processes such as Raman scattering, fluorescence quenching, photoinhibition, and photoadaptation must also be considered.

Raman scattering is wavelength dependent and occurs when radiative energy passing through a transparent medium undergoes an inelastic collision and exchanges a small amount of energy with the scattering molecules. The change in energy corresponds to a vibrational or rotational energy transition within the scattering molecule and to an increase or a decrease in the frequency of the scattered photon (Slayter, 1976). An increase in frequency occurs when the scattering molecule exists in an excited state and the collision causes energy to be transferred to the scattered photon. A scattered photon undergoes a decrease in frequency when the collision imparts the photon's incident energy to the scattering molecule which is then elevated to an excited state. It is this lower energy, scattered photon that may cause errors in fluorescence interpretations.

When a narrow band excitation filter is used, care must be taken not to accept the corresponding Raman peak as a significant fluorescence signal. With broad band excitation, a level of background Raman fluorescence over a broader range of wavelengths will be present. For water, Raman scattering is calculated by the following equations in terms of wave number (cm^{-1}):

$$\frac{1}{\lambda_r} = \frac{1}{\lambda_{ex}} - 3600 \qquad (2)$$

or in terms of wavelength (nm):

$$\lambda_r = \left[\frac{1}{\lambda_{ex}} - (3.6*10^{-4}) \right]^{-1} \qquad (3)$$

where λ_r is the Raman wavelength and λ_{ex} is the excitation wavelength (Lakowicz, 1983). Since broad band excitation (Fig. 6) was used during VERTEX 7, background fluorescence due to Raman scattering occurred from 382 to 719 nm.

Fluorescence quenching results in a decrease in fluorescence intensity, and, among other processes, occurs when molecular oxygen is in direct contact with the fluorescing molecule (Kautsky, 1939; Lakowicz, 1983). Oxygen is paramagnetic, which means that it has an unpaired electron in its natural state, and is a scavenger for weakly bound single electrons, such as those that occur when a fluorescent molecule is excited. The pairing of the single electrons from oxygen and from the excited molecule effectively decreases the fluorescent capabilities of that molecule. The relative positions of maxima and minima, therefore, must be taken into account when oceanic fluorescence signals are strongly associated with low concentrations of dissolved oxygen.

Photoinhibition generally refers to a depression in photosynthetic capacity due to super-saturating levels of irradiance. The damage to the photosynthetic apparatus caused by high radiation levels may sometimes be

reversible. During photoinhibition, relatively less of the absorbed energy can be used for photosynthesis, and the excess energy is dissipated as heat or fluorescence. If heat is the primary means for releasing the excess energy, fluorescence decreases. In contrast, if the excess energy is primarily reemitted as light, then photoinhibition results in an increase in fluorescence. Photoinhibition studies have shown depressed *in situ* chlorophyll *a* fluorescence in phytoplankton from the Gulf of California (Kiefer, 1973a) and increased phycoerythrin fluorescence in *Synechococcus* clone WH 7803 (Barlow and Alberte, 1985). Thus, the intensity of photoinhibited fluorescence is either reduced or augmented in comparison with the fluorescence of an undamaged photosystem under the same environmental conditions.

Photoadaptation involves intracellular control of pigment concentration and distribution, and occurs in response to fluctuations in nutrient and light levels. Increases in chlorophyll *a* per cell were observed at both lower irradiances and nutrient replete conditions (Laws and Bannister, 1980; Kiefer and Kremer, 1981). Fluctuations in the distribution of chlorophyll *a* in dinoflagellates have been linked to circadian rhythms. Hardeland and Nord (1984) observed the expansion and contraction of chloroplasts in *Pyrocystis noctiluca*, and Fabros and Sweeney (1988) reported that chloroplasts in *Pyrocystis fusiformis* migrate toward

the cell's nucleus at dusk and away from the nucleus at dawn. In essence, photoadaptive differences in *in situ* chlorophyll *a* fluorescence signals are dependent upon the amount of chlorophyll *a* exposed to excitation wavelengths.

Fluorescence vs. Total Attenuation

Pak *et al.* (1988) present a model using the CF:SPM ratio to explain observed c and CF patterns in the upper 250 m of the water column near 150 W. The basis of Pak *et al's* model is the assumption that c and CF patterns are determined by phytoplankton response to variations in the availability of light and nutrients. VERTEX 7 data are discussed in terms of this model and, in an attempt to better understand the interrelationships between F and c, are presented in the form of scatter plots similar to fluorescence/scatter correlations used in flow cytometry (Yentsch *et al.*, 1983).

According to Pak *et al's* model, F and c are related by the pigment to SPM ratio. These ratios are summarized into the principal patterns observed during VERTEX 7 (Fig. 18):

1) For a nutrient limited environment (oligotrophic gyre), F and c are relatively low at the surface. Little change in c occurs relative to the changes observed in F.

2) In regions where light limitations are nearly matched by low nutrient concentrations, the pattern contains two areas where F and c are positively correlated. This suggests that increases or decreases in particles and pigments occur with a constant ratio.

3) In a light limited environment where nutrients are abundant (subarctic waters), both F and c are relatively high at the surface and small changes in F occur in comparison to the changes observed in c.

4) The last relationship involves changes in c while F is constant and near its lowest value. This pattern indicates variations in concentrations of non-fluorescent particles, such as organisms without chlorophyll or phycoerythrin, or sediments from the benthic boundary layer.

In addition, the model predicts that the depth of the euphotic zone is indicated by the inflection point where both F and c begin to decrease concomitantly.

Primary Maximum. South of the frontal system at 33° N, CF increased from the surface to 140 m then decreased to its lowest value at 240 m. Concentration of particles, in terms of c, continuously decreased over the same depth range (Fig. 19a). The pattern for this F:c ratio is

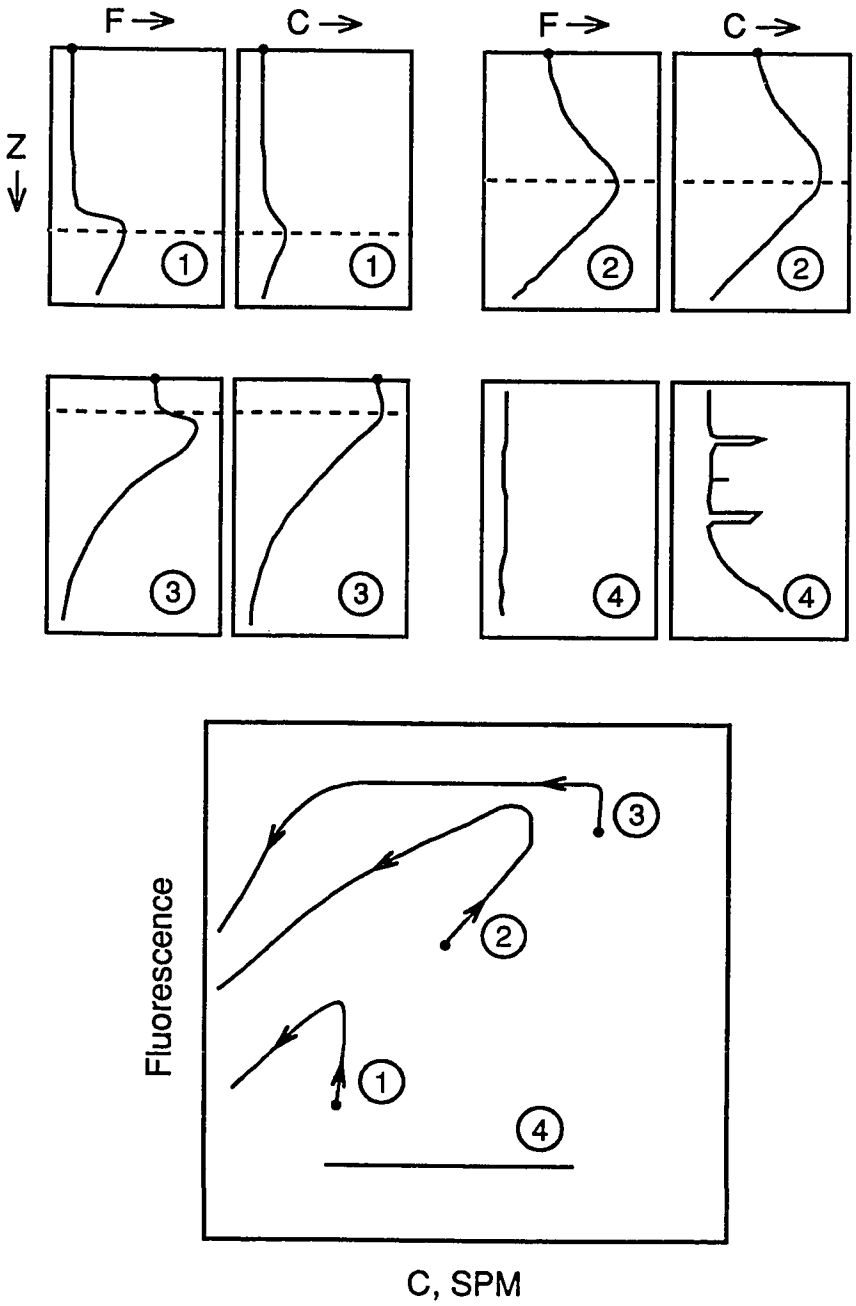

Figure 18. Diagnostic diagram for log-scaled fluorescence vs. total attenuation correlations. Patterns represent nutrient limited conditions (1), frontal region with the nutricline in the euphotic zone (2), light limited conditions (3), and the effects of non-fluorescent particles (4).

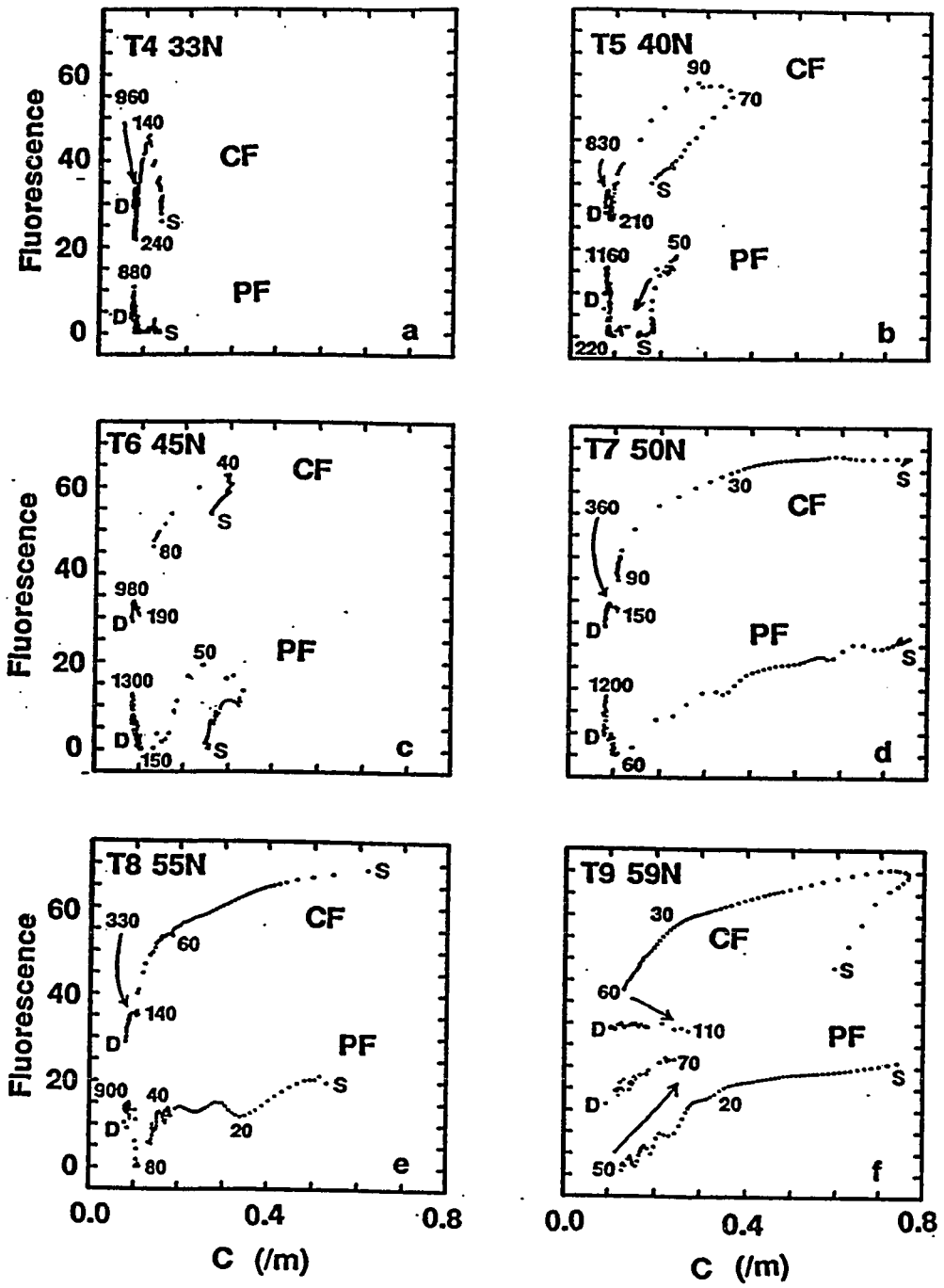

Figure 19. Fluorescence and total attenuation plots for major VERTEX 7 stations. Note that chlorophyll (CF) and phycoerythrin (PF) fluorescence units are observed (i.e. log-scaled) values interpolated to 0.1° C intervals. Depths (m) of significant inflection points are indicated, with S=sea surface and D=2000 m except at 59° N where D=970 m.

indicative of nutrient limitation (pattern 1, Fig. 18) and is also in good agreement with Pak *et al's* (1988) data for oligotrophic waters at 28° N. In contrast, there was essentially no PF in the shallow water column at 33° N (pattern 4).

In the subarctic front (40° N) and south of the Alaska Gyre (45° N), pattern 2 was dominant for both CF and PF (Figs. 19b, c). At 45° N, both nutrient data and secchi depth were collected. Between the surface and 50 m, $NO_3^=$ concentrations increased from 5.57 to 9.37 μmoles kg^{-1} (Martin *et al.*, 1989), and the base of the euphotic zone was estimated at 60 m from a secchi depth of 22 m. The inflection at 40 m for CF and at 50 m for PF indicates limiting conditions. Since these depths were slightly shallower than the depth of the euphotic zone, light and nutrient limitations were nearly balanced. Thus, pattern 2 represents intermediate conditions between nutrient limited and light limited environments. This pattern is not discussed by Pak *et al.* (1988).

North of 45° N, pattern 3 was dominant in CF and PF at 50° and 55° N (Figs. 19d, e), indicating a region where nutrients were in excess and light was the limiting factor. The CF data at these two locations were also comparable to the subarctic data at 42° N shown by Pak *et al.* (1988). At 59° N, only pattern 3 occurred for PF while a combination of patterns 2 and 3 was evident for CF (Fig. 19f). The near-

surface (0-10 m) CF:c correlation (pattern 2) does not indicate either nutrient or light limitations. This is interesting because the nitrate concentration for 5 m at this station was at or below detection limits (Martin *et al.*, 1989) and the concentration of particles extrapolated from c was relatively high. A possible explanation for this shallow CF:c pattern is photoinhibition. The near-surface CF data were obtained near 13:45 local time (Table 1). Conceivably, irradiance levels at that time were photoinhibiting, causing a depression in CF signals to 10 m.

Since fluorescence is only an indirect method of detecting the presence of pigments, identification of the organisms sensed by the fluorometer is speculative; however, phycoerythrin occurs only in red algae, cryptomonads, and cyanobacteria (Stewart and Farmer, 1984; MacColl and Guard-Friar, 1987). In addition to chlorophyll and phycoerythrin, cryptophytes also contain the carotenoids α-carotene and alloxanthin (Kirk, 1983). Since pigment analyses at 50° N showed negligible concentrations of alloxanthin (Welschmeyer, pers. comm.) and since Booth (1988) reported the presence of the cyanobacterium *Synechococcus* in the subarctic Pacific, the PF observations of VERTEX 7 were most likely due to cyanobacteria. Plankton samples from VERTEX 7 contained diatoms, coccolithophores, and dinoflagellates (Martin *et al.*, 1989), all of which would account for the CF observations.

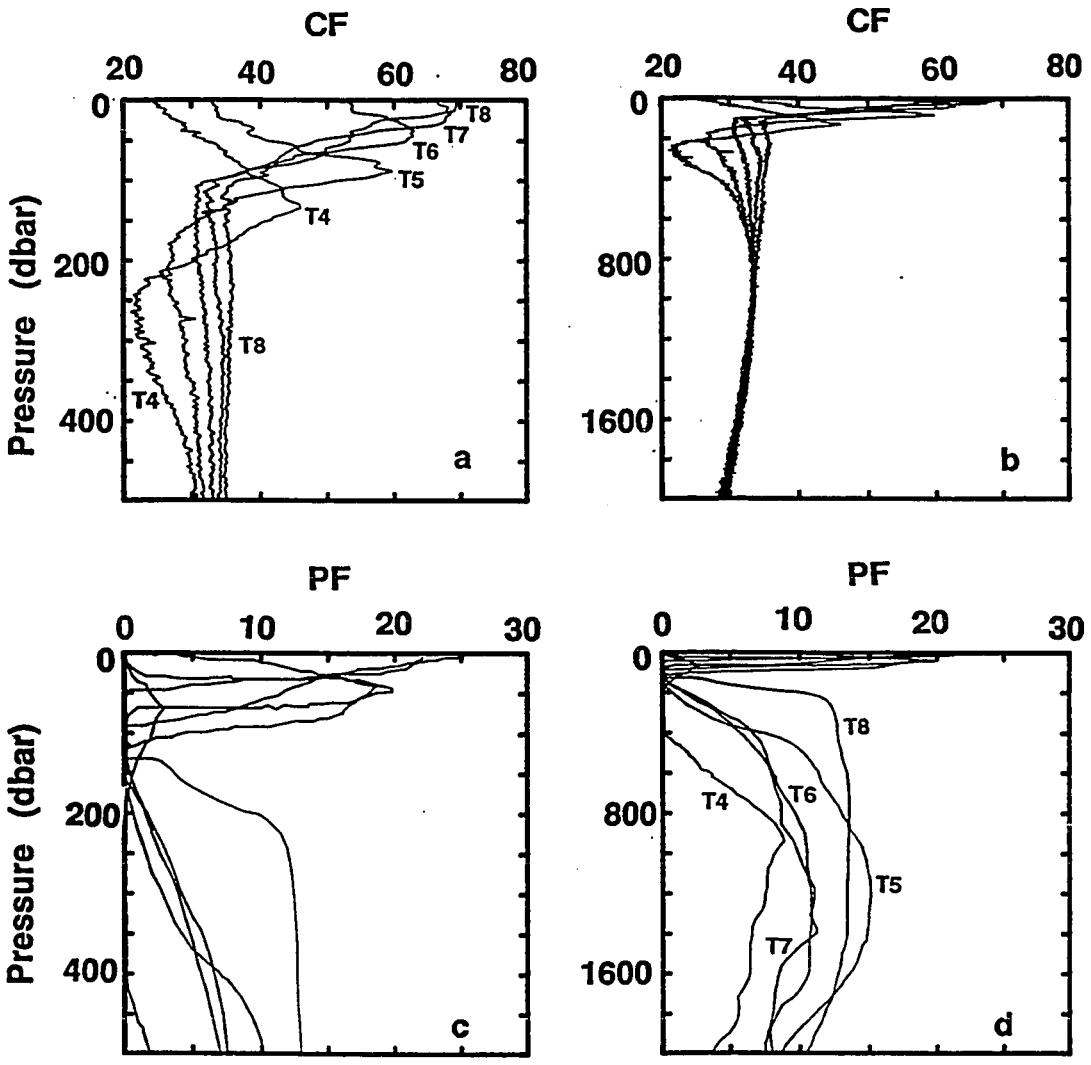

Figure 20. Observed (i.e. log-scaled) chlorophyll (CF) and phycoerythrin (PF) fluorescence profiles at major VERTEX 7 stations. a) Observed CF to 500 m. b) Observed CF to 2000 m. Note shoaling and filling of the CF minimum. c) Smoothed PF to 500 m. d) Smoothed PF to 2000 m.

Fluorescence Minimum. In oligotrophic waters (33° N), well developed CF and PF minima were observed while in eutrophic waters (55° N), only the intensity of the PF minimum was maintained (Fig. 20). Examination of the data showed that the CF tertiary maximum value of 34 fluorescence units (FU) at 800 m was sustained throughout the transect and that the minimum CF value of 22 FU at 33° N steadily increased to 33 FU at 55° N.

At 33° N, the fluorescence minimum occurred from 200 to 300 m. This depth interval is within the vertical migration depth range of zooplankton (Longhurst and Harrison, 1989) and the zone occasionally populated by suspension feeders such as giant larvaceans (Silver, pers. comm.; Barham, 1979). These larvaceans secrete mucus houses, up to 1 m in diameter, which effectively filter very small particles. This scenario suggests that the fluorescence minimum may not represent a lack of fluorescent organic particles, but may be the result of these particles being "repackaged" inside the gut of zooplankton.

The formation of a pigment minimum is enhanced by low surface production, by slow downward transport, and by relatively effective grazing. Unlike CF, the PF distribution showed a strong minimum at all stations (Fig. 20c), indicating that chlorophyll and phycoerythrin containing particles are produced and consumed by different processes. If phycoerythrin is contained in only small

(1 μm), slowly sinking particles (e.g. unicellular cyanobacteria) and chlorophyll is contained predominantly in larger, quickly sinking particles (e.g. diatoms), then suspension feeders, such as larvaceans, as well as macrozooplankton, via the microbial loop (Azam *et al.*, 1983; Jumars *et al.*, 1989), may graze phycoerythrin containing organisms to low levels more effectively than the larger sized algal cells.

Tertiary Maximum. Although the CF and PF signals in the tertiary maximum were relatively weak in comparison to those of the primary maximum, the tertiary maximum was not an artifact of Raman scattering since lowest CF values were seen at 33° N and lowest PF values were observed throughout the transect in the overlying fluorescence minimum. This deep feature was also not due to reduced quenching related to low dissolved oxygen concentrations. Examination of the data showed that the core of the oxygen minimum was not coincident with the fluorescence maxima at intermediate depths. In addition, both CF and PF tertiary maxima began to steeply shoal at 50° N to about 150 m at 59° N while the oxygen minimum remained near 1000 m.

All of the intermediate depth tertiary maximum F:c correlations followed pattern 1 (Fig. 20); however, the biological interpretations based upon these observations are not as straightforward as those for the primary maximum.

The interpretation of the fluorescence minimum clearly differentiated the CF from the PF tertiary maximum. The filling in of the overlying CF minimum and the constant intensity of the CF signals at intermediate depth clearly showed that the appearance of a CF tertiary maximum was dependent upon the maintenance of the CF minimum. The tertiary PF feature was, however, a true maximum since the PF minimum was maintained throughout the transect.

Although data at 59° N did not extend to 2000 m, there was a significant relationship between F and c. In both cases, an abrupt increase in c occurred at 110 and 70 m for CF and PF, respectively (Fig. 19f). The CF relationship showed pattern 4 while the PF ratios showed a slightly positive correlation. In relation to CF, the pattern indicated resuspension of continental margin sediments or the presence of nonchlorophyll containing organisms. On the other hand, the PF pattern indicated that the sediments might be a source of phycoerythrin containing particles.

Chlorophyll vs. Phycoerythrin Fluorescence

In an attempt to further characterize the primary and tertiary fluorescence maxima, a diagnostic diagram (Fig. 21) using CF and PF correlations was developed. Correlation plots between CF and PF are similar to flow cytometry diagrams (Olson *et al.*, 1985; Wood *et al.*, 1985; Chisholm *et al.*, 1986) with the exception that each point in the

correlation plots represents an assemblage of particles at a single depth, while each point in flow cytometry diagrams represents a single cell. Patterns in the diagnostic diagram (Fig. 21) are as follows:

A) Populations in which CF is low and constant while PF varies.

B) Populations with variable CF and constant, low PF.

C) Covariation between CF and PF.

Primary Maximum. Central gyre surface waters (Fig. 22a) appeared to be chlorophyll dominant, pattern B, while the subarctic surface waters (Fig. 22d-f) appeared to have a more or less fixed ratio of CF to PF, pattern C. These fluorescence observations indicate the presence of chlorophyll, phycoerythrin and/or "chlorophyll-like" pigments. Diatoms, coccolithophores, and dinoflagellates contain chlorophyll but not phycoerythrin. *Synechococcus* sp. contains both chlorophyll and phycoerythrin (Waterbury *et al.*, 1979). Prochlorophytes, which are smaller than unicellular cyanobacteria and contain divinyl chlorophyll (Chisholm *et al.*, 1988; Olson *et al.*, 1990b) but not phycoerythrin, were recently identified in the subtropical North Pacific (Chisholm *et al.*, 1988). Thus, the observed near-surface fluorescence signatures were consistent with plankton populations of non-phycoerythrin bearing algae and

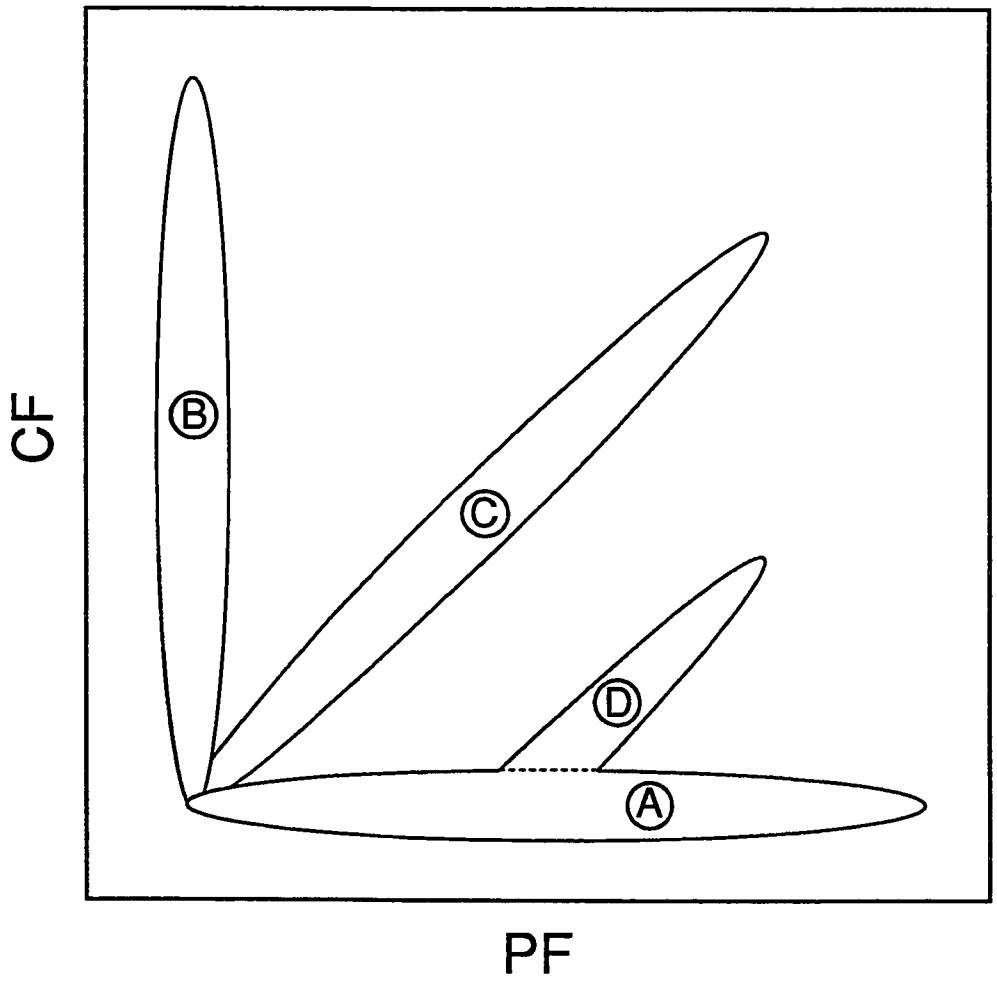

Figure 21. Diagnostic diagram for chlorophyll (CF) vs. phycoerythrin (PF) fluorescence (log-scaled) correlations. Patterns represent phycoerythrin dominant populations (A), chlorophyll dominant populations (B), populations with a fixed ratio of chlorophyll to phycoerythrin (C), and photic zone *Synechococcus* sp. flow cytometry observations (D) of Chisholm *et al.* (1986).

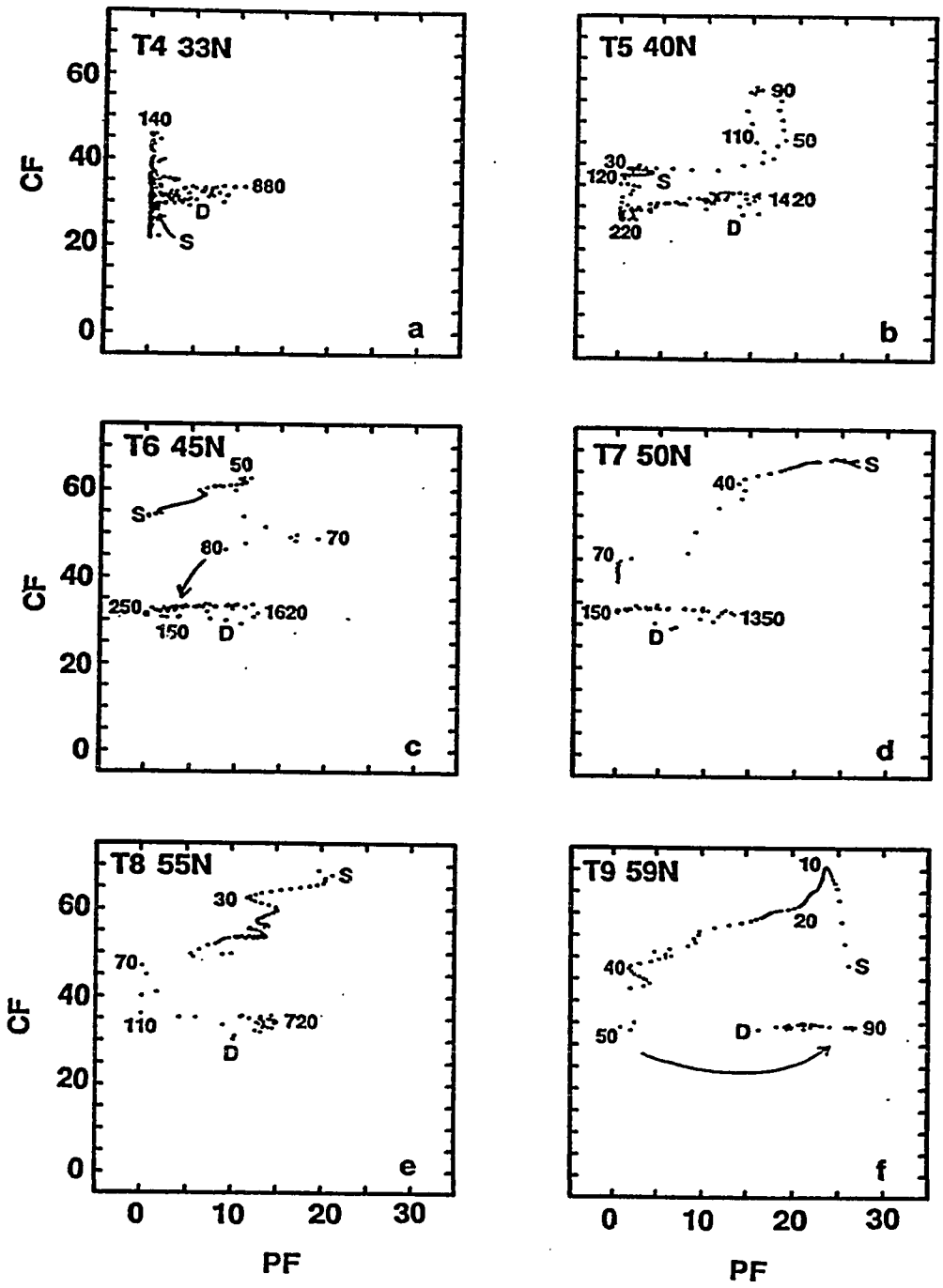

Figure 22. Chlorophyll (CF) and phycoerythrin (PF) fluorescence correlations for major VERTEX 7 stations. Note that CF and PF are observed (i.e. log-scaled) values interpolated to 0.1° C intervals. Depths (m) of significant inflection points are indicated with S=sea surface and D=2000 m except at 59° N where D=970 m.

prochlorophytes in the central gyre as well as *Synechococcus* in the subarctic.

Tertiary Maximum. In contrast to the correlations for the primary maximum, the tertiary fluorescence maximum stands out as a solitary feature. Pattern A was characteristic of the tertiary maximum and was found in the deeper waters at all stations (Fig. 22). Intermediate depth waters, therefore, contain populations having constant and low CF with varying PF.

The release of fecal materials, rich in partially digested, but viable, algal cells and cyanobacteria, may be responsible for the tertiary fluorescence maximum. Work by Porter (1976) shows that algal cells with sheaths are not always completely digested by zooplankton. Arnold (1971) has shown that in some cases, cyanobacteria are unpalatable as well as indigestible. From the evidence discussed above, the deep fluorescence feature may be caused by either free-living or detrital assemblages of cyanobacteria that do not contain appreciable amounts of chlorophyll.

Observations of CF were relatively less noisy than PF at depth (Fig. 23), and this difference between CF and PF may reflect the source of these signals. The work of Silver *et al.* (1986) provides an explanation for tertiary fluorescence maximum observations. Silver *et al.* (1986) indicate two types of cell populations found in the deep

sea: 1) those present on rapidly sinking particles such as fecal pellets and marine snow (detrital aggregates > 0.5 mm) or on smaller, slowly sinking detrital particles; or 2) suspended cells. They found the cells associated with particles to be ultrastructurally intact. This suggests that these cells were quickly transported to depth and that those affiliated with fecal pellets were indigestible (Arnold, 1971; Porter, 1976; Johnson *et al.*, 1982). Cyanobacteria are prominent occupants of detrital material, marine snow, and fecal pellets (Silver *et al.*, 1986; Lochte and Turley, 1988), all of which are relatively large sized particles. These larger particles contain upwards of 10^4 cells mm^{-1} and are encountered more sporadically by fluorometer than are free-living suspended cells. Hence, a single large particle in the fluorometer's field of view produces a fluorescence spike, resulting in a noisy signal. The observation that CF is not as noisy argues that these detrital aggregates are richer in cyanobacterial cells than in eukaryotic or prochlorophyte cells.

Silver and her coauthors (1986) also suggest that the presence of cyanobacteria at depth could be explained by heterotrophic growth, an hypothesis they note is not yet supported by experiment. However, the low, constant CF with varying PF pattern implies that the tertiary feature does not just reflect pigments from organisms transported downward from the euphotic zone. For many years,

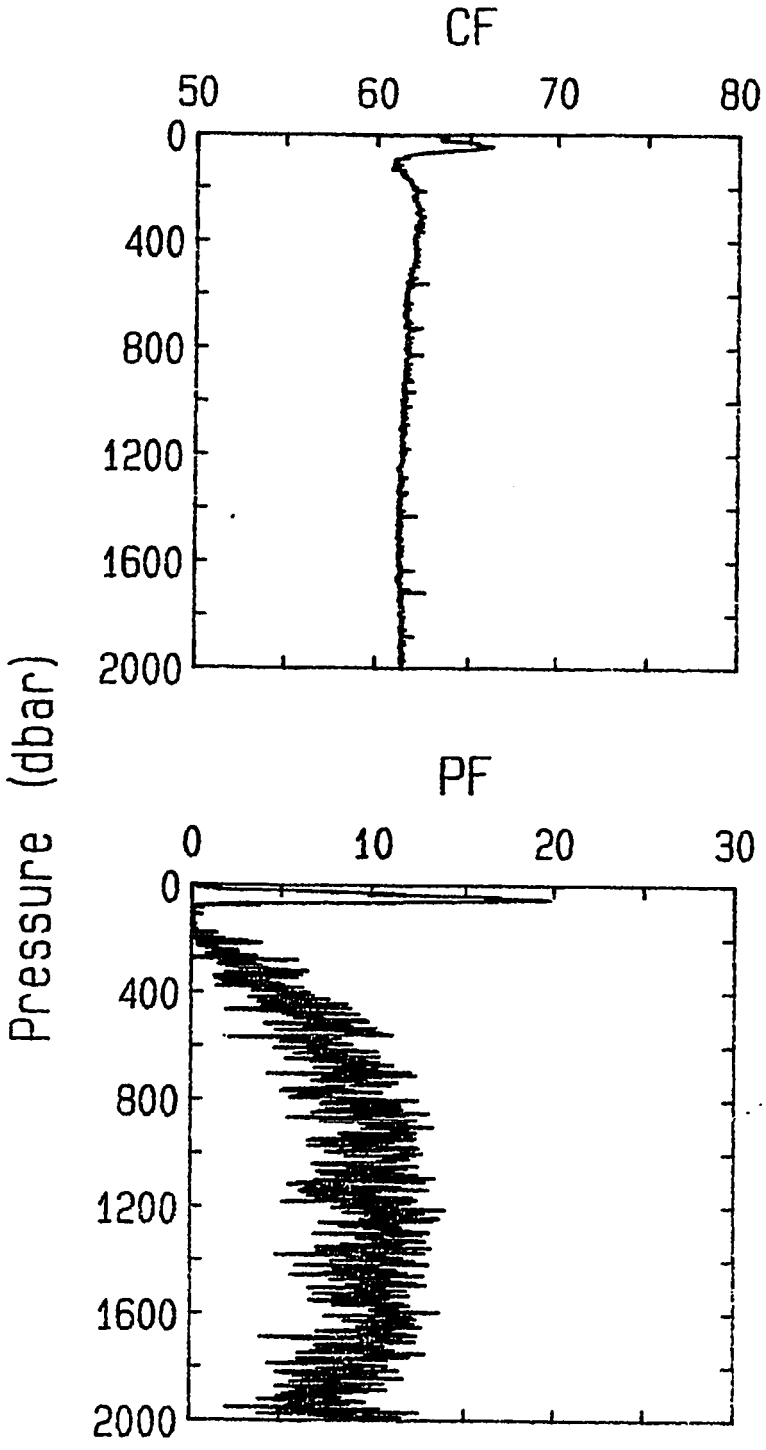

Figure 23. Fluorescence (log-scaled) profiles to 2000 m for chlorophyll (a) and phycoerythrin (b). Note the difference in the signal noise levels.

cyanobacteria were considered to be obligate aerobic photoautotrophs, but some are now known to be capable of aphotic, heterotrophic growth (Carr and Wyman, 1986).

Unlike photoautotrophy, heterotrophy does not require chlorophyll for survival. Recent research (Cohen-Bazire and Bryant, 1982; Wyman *et al.*, 1985; Kromkamp, 1987; Kramer *et al.*, 1988) indicates that phycobiliproteins, such as phycoerythrin, not only function as photosynthetic light harvesters, but may also serve as nitrogen storage compounds. It is also well established that cyanobacteria require iron, as well as other trace metals, for their metabolism (Rueter and Petersen, 1987), and Martin *et al.* (1989) point out that Fe has a nutrient-like distribution with depth. Furthermore, Sugimura and Suzuki (1988) show a strong inverse correlation between dissolved organic carbon (DOC) and apparent oxygen utilization (AOU) with depth. All of these findings support the hypothesis that the deep fluorescence signature in the North Pacific may be an indicator of a viable, perhaps slow growing, cyanobacteria population.

CONCLUSIONS

Near-surface chlorophyll fluorescence signals are commonly attributed to phytoplankton, such as diatoms, coccolithophores, and dinoflagellates. The recent discovery of a free-living prochlorophyte, containing divinyl chlorophyll, in the tropical Pacific euphotic zone (Chisholm *et al.*, 1988), however, suggests that prochlorophytes may also contribute to the primary chlorophyll fluorescence maximum in the Gulf of Alaska.

Based upon the observations of this study and the work of Booth (1988) and Welschmeyer (pers. comm.), the primary phycoerythrin fluorescence maximum indicates that cyanobacteria, probably *Synechococcus*, are abundant in the euphotic zone of the subarctic Pacific and are associated with cooler rather than warmer water temperatures. Thus, the spatial extent of *Synechococcus* in the North Pacific Ocean may be more widespread than was previously thought.

Differences between the chlorophyll and phycoerythrin fluorescence minima in the Gulf of Alaska indicate dissimilar grazing pressures on chlorophyll and phycoerythrin containing organisms. The prominent, widespread phycoerythrin fluorescence minimum contributes toward the appearance of the tertiary phycoerythrin fluorescence maximum throughout the Northeast Pacific Ocean.

The tertiary fluorescence signature indicates the presence of particles more heavily pigmented with

phycoerythrin than chlorophyll *a* within the oxygen minimum zone. Phycoerythrin containing organisms, probably cyanobacteria, in the overlying fluorescence maximum were effectively grazed in the fluorescence minimum. Hence, ultrastructurally intact cyanobacterial cells were probably transported to depth via fecal pellets (Arnold, 1971; Johnson *et al.*, 1982; Silver *et al.*, 1986). Since some cyanobacteria are capable of facultative chemoheterotrophic growth in the dark (Rippka, 1972), and combined with the fact that phycoerythrin may act as a reservoir for nitrogen (Cohen-Bazire and Bryant, 1982; Kramer *et al.*, 1988), that dissolved organic carbon is inversely correlated with apparent oxygen utilization (Sugimura and Suzuki, 1988), and that iron increases with depth (Martin *et al.*, 1989), the presence of heterotrophic cyanobacteria at intermediate depths in the Northeast Pacific Ocean is a distinct possibility.

BIBLIOGRAPHY

Alberte, R.S., A.M. Wood, T.A. Kursar, and R.R.L. Guillard (1984) Novel phycoerythrins in marine *Synechococcus* spp. Plant Physiology 75:732-739.

Algarra, P., M. Estrada, and F.X. Niell (1988) Phycobiliprotein distribution across the western Mediterranean divergence. Deep-Sea Research 35(8)1425-1430.

Anderson, G.C. (1969) Subsurface chlorophyll maximum in the Northeast Pacific Ocean. Limnology and Oceanography 14(3)386-390.

Anderson, G.C. (1972) Double oxygen minimum in the southeastern Pacific Ocean. Journal of Marine Research 30(3)275-280.

Andrews, C.C., D.M. Karl, L.F. Small, and S.W. Fowler (1984) Metabolic activity and bioluminescence of oceanic faecal pellets and sediment trap particles. Nature 307(5951)539-540.

Arnold, D.E. (1971) Ingestion, assimilation, survival, and reproduction by *Daphnia pulex* fed seven species of blue-green algae. Limnology and Oceanography 16:906-920.

Austin, R.W. and T.J. Petzold (1977) Considerations in the design and evaluation of oceanographic transmissometers. *In* Light in the sea. J.E. Taylor (Ed.). Dowden, Hutchinson and Ross, Inc. Pennsylvania. pp. 104-120.

Azam, F., T. Fenchel, J.G. Field, J.S. Gray, L.A. Meyer-Reil, and F. Thingstad (1983) The ecological role of water-column microbes in the sea. Marine Ecology Progress Series 10:257-263.

Barham, E.G. (1979) Giant larvacean houses: Observations from deep submersibles. Science 204:1129-1131.

Barlow, R.G. and R.A. Alberte (1985) Photosynthetic characteristics of phycoerythrin-containing marine *Synechococcus* spp. 1. Responses to growth photon flux density. Marine Biology 86(1)63-74.

Bartz, R., J.R.V. Zaneveld, and H. Pak (1978) A transmissometer for profiling and moored observations in water. Ocean Optics V, Proceedings, Society of Photo-optical Instrumentation Engineering 160:102-108.

Bishop, J.K.B. (1986) The correction and suspended particulate matter calibration of Sea Tech transmissometer data. Deep-Sea Research 33:121-134.

Booth, B.C. (1988) Size classes and major taxonomic groups of phytoplankton at two locations in the subarctic Pacific Ocean in May and August, 1984. Marine Biology 97:275-286.

Broecker, W.W. and T.H. Peng (1982) Tracers in the sea. Eldigio Press. New York. 690 p.

Broenkow, W.W. (1982) A comparison between geostrophic and current meter results in a California Current eddy. Deep-Sea Research 29:1303-1311.

Broenkow, W.W., A.J. Lewitus, M.A. Yarbrough, and R.T. Krenz (1983) Particle fluorescence and bioluminescence distributions in the eastern tropical Pacific. Nature 302:329-331.

Broenkow, W.W., A.J. Lewitus, and M.A. Yarbrough (1985) Spectral observations of pigment fluorescence in intermediate depth waters of the North Pacific. Journal of Marine Research 43:875-891.

Broenkow, W.W., M.A. Yarbrough, and M.A. Yuen (1988) Oceanographic results from the VERTEX seasonal experiments. Moss Landing Marine Laboratories Technical Publication 88-1, Moss Landing, CA. 67 p.

Carr, N.G. and M. Wyman (1986) Cyanobacteria: their biology in relation to the oceanic picoplankton. *In* Photosynthetic picoplankton. T. Platt and W.K.W. Li (Eds.) Canadian Bulletin of Fisheries and Aquatic Sciences 214:159-204.

Chisholm, S.W., E.V. Armbrust, and R.J. Olson (1986) The individual cell in phytoplankton ecology: Cell cycles and applications in flow cytometry. *In* Photosynthetic picoplankton. T. Platt and W.K.W. Li (Eds.) Canadian Bulletin of Fisheries and Aquatic Sciences 214:343-369.

Chisholm, S.W., R.J. Olson, E.R. Zettler, R. Goericke, J.B. Waterbury, and N.A. Welschmeyer (1988) A novel free-living prochlorophyte abundant in the oceanic euphotic zone. Nature 334:340-343.

Cohen-Bazire, G. and D.A. Bryant (1982) Phycobilisomes: Composition and structure. *In* The biology of cyanobacteria. N.G. Carr and B.A. Whitton (Eds.) University of California Press. California. pp. 143-190.

Collins, D.J., D.A. Kiefer, J.B. SooHoo, and I.S. McDermid (1985) The role of reabsorption in the spectral distribution of phytoplankton fluorescence emission. Deep-Sea Research 32(8)983-1003.

Cuhel, R.L. and J.B. Waterbury (1984) Biochemical composition and short term nutrient incorporation patterns in a unicellular marine cyanobacterium, *Synechococcus* (WH7803). Limnology and Oceanography 29(2)370-374.

Cullen, J.J. (1982) The deep chlorophyll maximum: Comparing vertical profiles of chlorophyll *a*. Canadian Journal of Fisheries and Aquatic Sciences 39:791-803.

Denman, K.L. and A.E. Gargett (1988) Multiple thermoclines are barriers to vertical exchange in the subarctic Pacific during SUPER, May 1984. Journal of Marine Research 46(1)77-103.

Emerson, S. (1987) Seasonal oxygen cycles and biological new production in surface waters of the Subarctic Pacific Ocean. Journal of Geophysical Research 92(C6)6535-6544.

Eppley, R.W., E.H. Renger, E.L. Venrick, and M.M. Mullin (1973) A study of plankton dynamics and nutrient cycling in the central gyre of the North Pacific Ocean. Limnology and Oceanography 18(4)534-551.

Fabros, G.A. and B.M. Sweeney (1988) Chloroplast movement in a marine dinoflagellate, *Pyrocystis fusiformis*. Journal of Phycology 24:5.

Falkowski, P. and D.A. Kiefer (1985) Chlorophyll *a* fluorescence in phytoplankton: relationship to photosynthesis and biomass. Journal of Plankton Research 7(5)715-731.

Favorite, F., A.J. Dodimead, and K. Nasu (1976) Oceanography of the subarctic Pacific region, 1970-71. International North Pacific Fisheries Commission. Bulletin Number 33. 187 pp.

Frungel, F. and C. Koch (1980) A new *in situ* fluorometer for the measurement of fluorescent tracer substances with an exact logarithmic response over four decades. Meerestechurk Marine Technology 11:107-112.

Garfield, P.C., T.T. Packard, G.E. Friederich, and L.A. Codispoti (1983) A subsurface particle maximum layer and enhanced microbial activity in the secondary nitrite maximum of the northeastern tropical Pacific Ocean. Journal of Marine Research 41:747-768.

Gieskes, W.W. and G.W. Kraay (1986) Fluoristic and physiological differences between the shallow and the deep nanophytoplankton community in the euphotic zone of the open tropical Atlantic revealed by HPLC analysis of pigments. Marine Biology 91:567-576.

Gieskes, W.W.C., G.W. Kraay, and S.B. Tijssen (1978) Chlorophylls and their degradation products in the deep pigment maximum layer of the tropical North Atlantic. Netherlands Journal Sea Research 12(2)195-204.

Glover, H.E., L. Campbell, and B.B. Prezelin (1986) Contribution of *Synechococcus* spp. to size-fractioned primary productivity in three water masses in the Northwest Atlantic Ocean. Marine Biology 91:193-203.

Gowing, M.M. and M.W. Silver (1983) Origins and microenvironments of bacteria mediating fecal pellet decomposition in the sea. Marine Biology 73:7-16.

Hardeland, R. and P. Nord (1984) Visualization of free-running circadian rhythms in the dinoflagellate *Pyrocystis noctiluca*. Marine Behavior and Physiology 11:199-207.

Hayward, T.L. (1987) The nutrient distribution and primary production in the central North Pacific. Deep-Sea Research 34(9)1593-1627.

Hayward, T.L. and J.A. McGowan (1985) Spatial patterns of chlorophyll, primary production, macrozooplankton biomass, and physical structure in the central North Pacific Ocean. Journal of Plankton Research 7(2)147-167.

Hayward, T.L., E.L. Venrick, and J.A. McGowan (1983) Environmental heterogeneity and plankton community structure in the central North Pacific. Journal of Marine Research 41:711-729.

Hoejerslev, N.K. (1980) On the origin of yellow substance in the marine environment. Studies in Physical Oceanography 42:39-56.

Holm-Hansen, O., C.J. Lorenzen, R.W. Holmes, and J.D.H. Strickland (1965) Fluorometric determination of chlorophyll. Journal du Conseil, Conseil permanent International pour l'Exploration de la mer 30:3-15.

Holm-Hansen, O. (1969) Determination of microbial biomass in ocean profiles. Limnology and Oceanography 14(5)740-747.

Jerlov, N.G. (1976) Marine Optics. Elsevier Oceanography Series 14. Elsevier Scientific Publishing Co. Amsterdam. 231 p.

Johnson, P.W. and J.M. Sieburth (1979) Chroococcoid cyanobacteria in the sea: a ubiquitous and diverse phototrophic biomass. Limnology and Oceanography 24(5)928-935.

Johnson, P.W., H.S. Xu, and J.McN. Sieburth (1982) The utilization of chroococcoid cyanobacteria by marine protozooplankters but not by calanoid copepods. Annales de l'Institut Oceanographique 58:297-308.

Jumars, P.A., D.L. Penry, J.A. Baross, M.J. Perry, and B.W. Frost (1989) Closing the microbial loop: dissolved carbon pathway to heterotrophic bacteria from incomplete ingestion, digestion and absorption in animals. Deep-Sea Research 36:483-496.

Karl, D.M. (1982) Microbial transformations of organic matter at oceanic interfaces: A review and prospectus. EOS 63(5)138-142.

Karl, D.M. and G.A. Knauer (1984) Vertical distribution, transport, and exchange of carbon in the northeast Pacific Ocean: evidence for multiple zones of biological activity. Deep-Sea Research 31(3)221-243.

Karl, D.M., G.A. Knauer, J.H. Martin, and B.B. Ward (1984) Bacterial chemolithotrophy in the ocean is associated with sinking particles. Nature 309:54-56.

Karl, D.M., D.R. Jones, J.A. Novitsky, C.D. Winn, and P. Bossard (1987) Specific growth rates of natural microbial communities measured by adenine nucleotide pool turnover. Journal of Microbiological Methods 6:221-235.

Kautsky, H. (1939) Quenching of luminescence by oxygen. Transactions of the Faraday Society 35:216-219.

Kiefer, D.A. (1973a) Fluorescence properties of natural phytoplankton populations. Marine Biologe 22:263-269.

Kiefer, D.A. (1973b) Chlorophyll *a* fluorescence in marine centric diatoms: Responses of chloroplasts to light and nutrient stress. Marine Biology 23:39-46.

Kiefer, D.A. and J.N. Kremer (1981) Origins of vertical patterns of phytoplankton and nutrients in the temperate, open ocean: a stratigraphic hypothesis. Deep-Sea Research 28A(10)1087-1105.

Kirk, J.T.O. (1983) Light and photosynthesis in aquatic ecosystems. Cambridge University Press. New York. 401 p.

Kramer, C.J.M. (1979) Degradation by sunlight of dissolved fluorescing substances in the upper layers of the eastern Atlantic Ocean. Netherlands Journal Sea Research 13(2)325-329.

Kramer, J.G., I. Morris, M. Wyman, J. Newman, and N.G. Carr (1988) Regulation of rRNA synthesis and growth in the marine cyanobacterium *Synechococcus* sp. WH 7803. First International Symposium on Marine Molecular Biology, October 9-11, 1988. Balitimore, Maryland.

Kromkamp, J. (1987) Formation and functional significance of storage products in cyanobacteria. New Zealand Journal of Marine and Freshwater Research 21:457-465.

Kursar, T.A., H. Swift, and R.S. Alberte (1981) Morphology of a novel cyanobacterium and characterization of light-harvesting complexes from it: Implications for phycobiliprotein evolution. Proc. Nat'l. Acad. Sci. 78(11)6888-6892.

Lakowicz, J.R. (1983) Principles of Fluorescence Spectroscopy. Plenum Press. New York. 496 p.

Laws, E.A. and T.T. Bannister (1980) Nutrient and light-limited growth of *Thalassiosira fluviatilis* in continuous culture, with implications for phytoplankton growth in the ocean. Limnology and Oceanography 25:457-473.

Lewitus, A.J. and W.W. Broenkow (1985) Intermediate depth pigment maxima in oxygen minimum zones. Deep-Sea Research 32(9)1101-1115.

Li, W.K.W. and A.M. Wood (1988) Vertical distribution of North Atlantic ultraphytoplankton: analysis by flow cytometry and epifluorescence microscopy. Deep-Sea Research 35(9)1615-1638.

Lochte, K. and C.M. Turley (1988) Bacteria and cyanobacteria associated with phytodetritus in the deep sea. Nature 333:67-69.

Loftus, M. E. and J. H. Carpenter (1971) A fluorometric method for determining Chlorophylls *a*, *b*, and *c*. Journal of Marine Research 29(3)319-338.

Lohrenz, S.E., D.A. Wiesenburg, I.P. DePalma, K.S. Johnson, and D.E. Gustafson, Jr. (1988) Interrelationships among primary production, chlorophyll, and environmental conditions in frontal regions of the western Mediterranean Sea. Deep-Sea Research 35(5)793-810.

Longhurst, A.R. and W.G. Harrison (1989) The biological pump: profiles of plankton production and consumption in the upper ocean. Progress in Oceanography 22:47-123.

Lynn, R.J. (1986) The subarctic and northern subtropical fronts in the eastern North Pacific Ocean in spring. Journal of Physical Oceanography 16(2)209-222.

MacColl, R. and D. Guard-Friar (1987) Phycobiliproteins. CRC Press, Inc. Florida. 218 p.

Martin, J.H. and G.A. Knauer (1983) VERTEX: Manganese transport with $CaCO_3$. Deep-Sea Research 30:411-425.

Martin, J.H., G.A. Knauer, W.W. Broenkow, K.W. Bruland, D.M. Karl, L.F. Small, M.W. Silver, and M.W. Gowing (1983) Vertical transport and exchange of materials in the upper waters of the oceans (VERTEX): Introduction to the program, hydrographic conditions, and major component fluxes during VERTEX 1. Moss Landing Marine Laboratories Technical Publication 83-2. Moss Landing, CA. 40 p.

Martin, J.H., G.A. Knauer, D.M. Karl, and W.W. Broenkow (1987) VERTEX: carbon cycling in the northeast Pacific. Deep-Sea Research 34(2)267-285.

Martin, J.H. and S.E. Fitzwater (1988) Iron deficiency limits phytoplankton growth in the north-east Pacific subarctic. Nature 331(6154)341-343.

Martin, J.H. and R.M. Gordon (1988) Northeast Pacific iron distributions in relation to phytoplankton productivity. Deep-Sea Research 35(2)177-196.

Martin. J.H., R.M. Gordon, S.E. Fitzwater, and W.W. Broenkow (1989) VERTEX: phytoplankton/iron studies in the Gulf of Alaska. Deep-Sea Research 36:649-680.

Megard, R.O., T. Berman, P.J. Curtis, and P.W. Vaughan (1985) Dependence of phytoplankton assimilation quotients on light and nitrogen source: implications for oceanic primary productivity. Journal of Plankton Research 7(5)691-702.

Mitchell, B.G. and D.A. Kiefer (1988) Chlorophyll *a* specific absorption and fluorescence excitation spectra for light-limited phytoplankton. Deep-Sea Research 35(5)639-663.

Morel, A. (1973) Diffusion de la lumiere par les eaux de mer. Resultats experimentaux et approache theorique. *In* Optics of the sea. AGARD Lecture Series No. 61. NATO Advisory Group for Aerospace Research and Development. pp. 3.1-32 to 3.1-61.

Morel, A. and L. Prieur (1977) Analysis of variations in ocean color. Limnology and Oceanography 22:709-722.

Moreth, C.M. and C.S. Yentsch (1970) A sensitive method for the determination of open ocean phytoplankton phycoerythrin pigments by fluorescence. Limnology and Oceanography 15(2)313-317.

Neale, P.J., J.J. Cullen and C.M. Yentsch (1989) Bio-optical inferences from chlorophyll *a* fluorescence: What kind of fluorescence is measured in flow cytometry? Limnology and Oceanography 34(8)1739-1748.

Olson, R.J., D. Vaulot, and S.W. Chisholm (1985) Marine phytoplankton distributions measured using shipboard flow cytometry. Deep-Sea Research 32:1273-1280.

Olson, R.J., S.W. Chisholm, E.R. Zettler, and E.V. Armbrust (1990a) Pigments, size, and distribution of *Synechococcus* in the North Atlantic and Pacific Oceans. Limnology and Oceanography 35:45-58.

Olson, R.J., S.W. Chisholm, E.R. Zettler, M.A. Altabet, and J.A. Dusenberry (1990b) Spatial and temporal distributions of prochlorophyte picoplankton in the North Atlantic Ocean. Deep-Sea Research 37:1033-1051.

Ong, L.J., A.N. Glazer, and J.B. Waterbury (1984) An unusual phycoerythrin from a marine cyanobacterium. Science 224:80-83.

Owens, W.B. and R.C. Millard (1985) A new algorithm for CTD oxygen calibration. Journal of Physical Oceanography 15:621-631.

Pak, H., D.A. Kiefer and J.C. Kitchen (1988) Meridional variations in the concentration of chlorophyll and microparticles in the North Pacific Ocean. Deep-Sea Research 35:1151-1171.

Porter, K.G. (1976) Enhancement of algal growth and productivity by grazing zooplankton. Science 192:1332-1334.

Prezelin, B.B., M. Putt, and H.E. Glover (1986) Diurnal patterns in photosynthetic capacity and depth-dependent photosynthesis-irradiance relationships in *Synechococcus* spp. and larger phytoplankton in three water masses in the Northwest Atlantic Ocean. Marine Biology 91:205-217.

Prieur, L. and S. Sathyendranath (1981) An optical classification of coastal and oceanic waters based on the specific spectral absorption curves of phytoplankton pigments, dissolved organic matter, and other particulate materials. Limnology and Oceanography 26(4)671-689.

Reeburgh, W.S. and G.W. Kipphut (1987) Chemical distributions and signals in the Gulf of Alaska, its coastal margins and estuaries *In* The Gulf of Alaska: Physical environment and biological resources. D.W. Hood and S.T. Zimmerman (Eds.). OCS study, MMS 86-0095.

Reid, J.L. and E. Shulenberger (1986) Oxygen saturation and carbon uptake near 28 N, 155 W. Deep-Sea Research 33(2)267-271.

Roden, G.I. (1975) On North Pacific temperature, salinity, sound velocity and density fronts and their relation to atmospheric forcing. Journal of Physical Oceanography 7:761-778.

Roden, G.I. (1977) Oceanic subarctic fronts of the Central Pacific: structure of and response to atmospheric forcing. Journal of Physical Oceanography 7(6)761-778.

Roden, G.I. (1980) On the subtropical frontal system north of Hawaii during winter. Journal of Physical Oceanography 10:342-362.

Rueter J.G. and R.R. Petersen (1987) Micronutrient effects on cyanobacterial growth and physiology. New Zeqaland Journal of Marine and Freshwater Research 21:435-445.

SCOR-UNESCO (1981) Tenth report of the joint panel on oceanographic tables and standards. UNESCO Technical Papers in Marine Science No. 35. 25 pp.

Sharp, J.H. (1983) The distribution of inorganic nitrogen and dissolved and particulate organic nitrogen in the sea. In Nitrogen in the marine environment. E.J. Carpenter and D.G. Capone (eds.) Academic Press. New York. pp. 1-36.

Shulenberger, E. (1978) The deep chlorophyll maximum and mesoscale environmental heterogeneity in the western half of the North Pacific central gyre. Deep-Sea Research 25:1193-1208.

Shulenberger, E. and J.L Reid (1981) The Pacific shallow oxygen maximum, deep chlorophyll maximum, and primary productivity, reconsidered. Deep-Sea Research 28A(9)901-919.

Silver, M.W., M.M. Gowing, and P.J. Davoll (1986) The association of photo-synthetic ultraplankton with pelagic detritus through the water column (0-2000 m). In Photosynthetic picoplankton. T. Platt and W.K.W. Li (Eds.) Canadian Bulletin of Fisheries and Aquatic Sciences 214:311-341.

Skoog, D.A. (1980) Principles of instrumental analysis. Saunders College Publishing. Philadelphia. pp. 225-246.

Slayter, E.M. (1976) Optical methods in biology. Robert E. Krieger Publishing Co. New York. 757 p.

Spinrad, R.W., H. Glover, B.B Ward, L.A. Codispoti, and G. Kullenberg (1989) Suspended particle and bacterial maxima in Peruvian coastal waters during a cold water anomaly. Deep-Sea Research 36:715-733.

Stanier, R.Y. (1977) The position of cyanobacteria in the world of phototrophs. Carlsberg Research Commun. 42(2)77-98.

Stewart, D.E. and F.H. Farmer (1984) Extraction, identification, and quantitation of phycobiliprotein pigments from phototrophic plankton. Limnology and Oceanography 29(2)392-397.

Strass, V. and J.D. Woods (1988) Horizontal and seasonal variation of density and chlorophyll profiles between the Azores and Greenland In Toward a theory on biological-physical interactions in the World Ocean. B. J. Rothschild, editor. Kluwer Academic Publishers. Dordrecht, The Netherlands. pp. 113-136.

Tully, J. P. and F.G. Barber (1960) An estuarine analogy in the subarctic Pacific Ocean. Journal Fish. Research Bd. Canada 17(1)91-112.

Venrick, E.L., J.A. McGowan, and A.W. Mantyla (1973) Deep maxima of photosynthetic chlorophyll in the Pacific Ocean. Fishery Bulletin 71:41-52.

Venrick, E.L. (1979) The lateral extent and characteristics of the North Pacific Central environment at 35 N. Deep-Sea Research 26A:1153-1178.

Venrick, E.L., J.A. McGowan, D.R. Cayan, and T.L. Hayward (1987) Climate and Chlorophyll *a*: Long-Term Trends in the Central North Pacific Ocean. Science 238:70-72.

Wastler, T.A. (1969) Spectral Analysis. Federal Water Pollution Control Administration. U.S. Department of the Interior. Washington, D.C. 99 pp.

Waterbury, J.B., S.W. Watson, R.R.L. Guillard, and L.E. Brand (1979) Widespread occurrence of a unicellular, marine, planktonic, cyanobacterium. Nature 277:293-294.

Wood, A. M. (1985) Adaptation of photosynthetic apparatus of marine ultraphytoplankton to natural light fields. Nature 316(6025)253-255.

Wood, A.M., P.K. Horan, K. Muirhead, D.A. Phinney, C.M. Yentsch, and J.B. Waterbury (1985) Discrimination between types of pigments in marine *Synechococcus* spp. by scanning spectroscopy, epifluorescence microscopy, and flow cytometry. Limnology and Oceanography 30:1303-1315.

Wyman, M., R.P.F. Gregory, and N.G. Carr (1985) Novel role for phycoerythrin in a marine cyanobacterium, *Synechococcus* strain DC2. Science 230:818-820.

Yarbrough, M.A., W.W. Broenkow, and R.E. Reaves (1989) An integral CTD rosette optical profiler. Marine Technology Society Journal 23:3-9.

Yentsch, C.M., P.K. Horan, K. Muirhead, Q. Dortch, E. Haugen, L. Legendre, L.S. Murphy, M.J. Perry, D.A. Phinney, S.A. Pomponi, R.W. Spinrad, A.M. Wood, C.S. Yentsch, and B.J. Zahuranec (1983) Flow cytometry and cell sorting: A technique for analysis and sorting of aquatic particles. Limnology and Oceanography 28(6)1275-1280.

Yentsch, C.S. and D.W. Menzel (1963) A method for the determination of phytoplankton chlorophyll and phaeophytin by fluorescence. Deep-Sea Research 10:221-231.

Yentsch, C.S. and C.M. Yentsch (1979) Fluorescence spectral signatures: the characterization of phytoplankton populations by the use of excitation and emission spectra. Journal of Marine Research 37(3)471-483.

Yentsch, C.S. and D.A. Phinney (1985) Spectral fluorescence: an ataxonomic tool for studying the structure of phytoplankton populations. Journal of Plankton Research 7(5)617-632.

APPENDIX 1

APPENDIX 1

In the past, interpretations of *in situ* dissolved oxygen distributions obtained from polarographic oxygen electrodes were difficult to make because temperature and pressure effects on membrane permeability were inadequately assessed. Prior to VERTEX 7, *in situ* oxygen observations were obtained with a Beckman oxygen electrode (Greene *et al.*, 1970). This electrode uses fixed circuitry to estimate membrane temperatures which leads to a large temperature time-lagged effect in areas of strong thermoclines and causes underestimation of downcast oxygen concentrations (Fig. 24a).

The algorithm developed by Owens and Millard (1985) attempts to correct the temperature time-lag response problem and is an alternative to the traditional method of correcting dissolved oxygen data via a least squares linear regression of bottle calibration samples. To correct for temperature and pressure affects on membrane permeability, the algorithm requires separate oxygen reduction current and electrode temperature measurements. For VERTEX 7, the Beckman oxygen electrode was modified by inserting a thermistor within 1 mm of the membrane, thereby decoupling the oxygen reduction current and electrode temperature signals.

The algorithm presented by Owens and Millard (1985) is of the following form:

$$O_2=[a+b(IO_2+\tau dIO_2/dt)]O_2'e[t_{cor}(T+w_t(T_o-T))+p_{cor}(P)] \quad (4)$$

where

a = oxygen reduction current intercept

b = oxygen reduction current slope

IO_2 = oxygen reduction current

τ = diffusive time constant

dIO_2/dt = diffusive rate across the membrane

O_2' = oxygen saturation as a f(S,T)

t_{cor} = temperature effect on membrane permeability

T = water temperature from CTD

w_t = weighting factor for electrode temperature

T_o = electrode temperature

p_{cor} = pressure effect on membrane permeability

P = pressure from CTD

The coefficients a, b, t_{cor}, and p_{cor} are determined by nonlinear regression between IO_2 and calibration samples. The weighting factor, w_t, is estimated by comparing the down- and upcast oxygen profiles. Application of w_t to downcast values adjusts the profile to median values for both the down- and upcasts.

The exponential term, $[t_{cor}(T+w_t(T_o-T))+p_{cor}(P)]$, corrects for temperature and pressure affects on membrane permeability. Owens and Millard use $w_t(T_o-T)$ to estimate

the temperature of the membrane; however, we assume that placement of a thermistor within 1 mm of the membrane adequately measures the membrane temperature. Thus, the term $w_t(T_o-T)$ is reduced to $w_t(T_o)$ with T_o now representing membrane temperature. Comparison of calibration oxygen samples with corrected electrode values (Fig. 24b) indicates that this modification does give a better estimate of the membrane temperature.

The CTDO profiler is lowered through the thermocline at slow winch speeds (10-15 $m \cdot min^{-1}$), which allows the oxygen electrode to cool. The diffusive terms, dIO_2 and τ, are effectively compensated for by this slow descent, and therefore, under these conditions, $\tau=0$.

Although the correcting algorithm by Owens and Millard (1985) has been, by necessity, altered, the values determined for a, b, t_{cor}, P_{cor}, and w_t are in line with those used by Owens and Millard (1985). The algorithm currently in use at Moss Landing Marine Laboratories is

$$O_2=(a+bIO_2)O_2'e[t_{cor}(T+w_t(T_o))+P_{cor}(P)] \qquad (5)$$

and coefficient values are listed in Table 2.

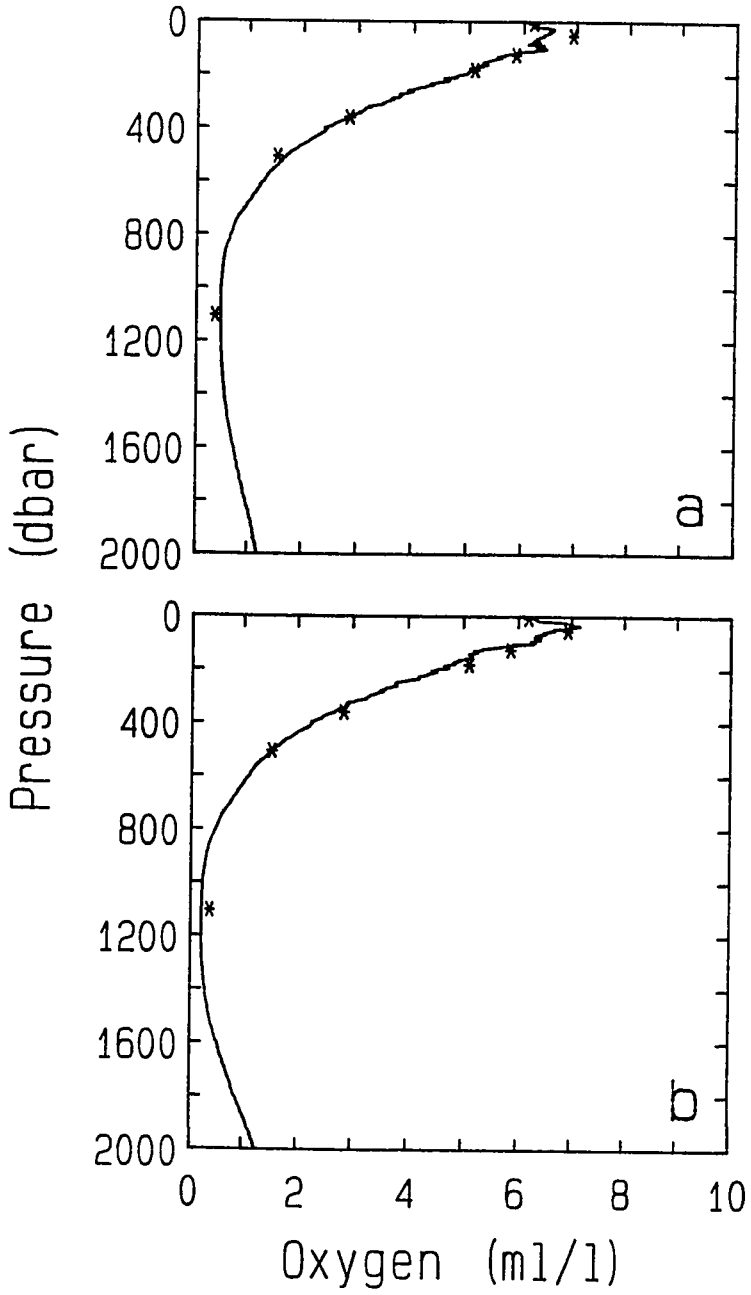

Figure 24. Dissolved oxygen ($ml \cdot l^{-1}$) profiles before use of the algorithm by Owens and Millard (a) and after use the the algorithm (b). * denotes bottle calibration values determined by modified Winkler titration.